HHS Public Access

Author manuscript

Sci Signal. Author manuscript; available in PMC 2015 June 16.

Published in final edited form as:

Sci Signal. ; 7(356): ra120. doi:10.1126/scisignal.2005948.

Npr2 regulates cellular utilization of glutamine for biosynthesis of nitrogen-containing metabolites through TORC1

Sunil Laxman[1], **Benjamin M. Sutter**[1], **Lei Shi**[1], and **Benjamin P. Tu**[1]

[1]Department of Biochemistry, UT Southwestern Medical Center, 5323 Harry Hines Blvd, Dallas, TX 75390-9038

Abstract

Cells must be capable of switching between growth and autophagy in unpredictable nutrient environments. Yeast cells lacking the conserved Iml1/Npr2/Npr3 complex (also called SEACIT), a negative regulator of TORC1, can bypass autophagy and proliferate during specific nutrient limitations. We determined that Npr2-deficient cells exhibit a metabolic state that is very distinct from WT cells under such limitations that demand oxidative metabolism. Instead of accumulating glutamine, *npr2*Δ cells consumed substantial amounts of glutamine to satisfy their demands for nitrogen, and maintained high S-adenosyl methionine (SAM) concentrations to fuel growth. Moreover, in normal cells, methionine addition stimulated glutamine consumption for synthesis of nitrogenous metabolites, showing how a sulfur amino acid cue is integrated with nitrogen utilization. These data reveal the metabolic basis by which the Iml1/Npr2/Npr3 complex regulates cellular homeostasis and demonstrate a key function for TORC1 in regulating the synthesis and utilization of glutamine as a nitrogen source.

Introduction

In normal cells, metabolism is closely regulated in tune with nutrient availability, providing anabolic substrates and energy for growth during nutrient sufficiency, while nutrient salvage processes such as autophagy are activated during starvations (1, 2). Imbalanced metabolic regulation can result in unchecked cell growth, as is often seen in cancer cells (3–5). In eukaryotes, the TORC1 pathway is a central nutrient-sensitive regulator of cell growth, responding particularly to amino acids (6–10). TORC1 activity is regulated in part by the conserved RAG family of GTPases (11–13), called Gtr1/2 in yeast (13), which are closely associated with the lysosome/vacuole as part of larger amino acid-sensing systems (11, 13).

Within this paradigm, a conserved protein complex consisting of Iml1, Npr2, and Npr3 (termed Npr2 complex) appears to be at the hub of amino acid sensing and cell growth regulation. Npr2 and Npr3 were first identified in *S. cerevisiae* as inhibitors of TORC1 activity, responding to nitrogen and amino acid signals (14–16). Along with Iml1, these proteins form a larger, vacuole-associated SEA complex (17, 18). Recent studies from yeast

Correspondence: benjamin.tu@utsouthwestern.edu.

Author contributions: The project was conceived by SL and BPT. Experiments were designed by SL and BPT, and executed by SL, BS and LS. The manuscript was written by SL and BPT.

and mammalian cells suggest that the Npr2 complex (also called SEACIT in yeast, and GATOR in mammals) inhibits TORC1 activity by negatively regulating the Gtr1/2 or RagA/B GTPases (19, 20). We previously observed that yeast cells induce autophagy when switched from rich to minimal medium containing lactate as the sole carbon source, in a manner dependent on the Npr2 complex (18). Interestingly, cells lacking any member of this complex escaped autophagy and instead continued to proliferate at a faster rate (18, 21). This phenotype is consistent with the proposal that Nprl2, the mammalian ortholog of yeast Npr2, is a potential tumor suppressor gene in cancers (22–24). Yet, precisely how the Npr2 complex regulates cellular metabolism and growth is unclear.

Herein, we define metabolic differences in Npr2-deficient yeast cells that allow them to continue proliferating under conditions where normal cells induce autophagy. Our results reveal the consequences of loss of a negative regulator of TORC1 under such a challenging nutrient environment and explain how the Npr2-complex regulates the TORC1 pathway to alter metabolic homeostasis.

Results

WT and *npr2*Δ cells growing in minimal lactate medium have contrasting metabolic states

When yeast cells growing in rich medium containing lactate as the sole carbon source (YPL) are switched to minimal, amino acid-free medium containing lactate (SL) at the same cell density, autophagy is induced (Fig. 1A) (18, 21). In contrast, *npr2*Δ cells bypassed autophagy under identical conditions (Fig. 1A), and proliferated at a faster rate than WT cells in SL medium (Fig. 1B), although this difference in proliferation was not observed in YPL (21). Such unchecked proliferation was not due to the accumulation of suppressor mutations (Fig. 1B). To compare the metabolic states of WT and *npr2*Δ cells under these conditions, which demand oxidative metabolism, we prepared extracts from cells switched to SL medium and measured relative metabolite amounts using targeted LC-MS/MS methods that simultaneously detect metabolites covering major metabolic pathways (Fig. 1C, Table 1). Both the direction and magnitude of changes of several metabolites were distinct in WT and *npr2*Δ cells (Fig. 1C), with several clusters of metabolites being anti-correlated (Fig. 1C, Table 1).

*npr2*Δ cells increase nitrogen assimilation and utilization for metabolite biosynthesis

We investigated whether specific metabolites explained the absence of autophagy and increased proliferation of *npr2*Δ cells. Since the amino acids leucine and isoleucine reportedly activate growth (13, 25), we asked if their abundance correlated with the increased growth of *npr2*Δ cells. Instead, we found that leucine amounts were lower in *npr2*Δ cells (Fig. S1, Table 1), which suggests alternate growth-inducing metabolic signals. However, we observed that glutamine increased in WT cells by >50-fold in ~5 h in SL medium (Fig. 2A), but remained low in *npr2*Δ cells. This suggested that *npr2*Δ cells either rapidly consumed glutamine, or synthesized glutamine at reduced rates in these conditions where ammonium was the sole nitrogen source.

Glutamine is a critical nitrogen donor for nucleotide (26), glutathione (27), and NAD^+ biosynthesis (28) (Fig. 2B), all of which may promote proliferation (29). In addition to satisfying cellular requirements for nitrogen, through anapleurosis glutamine can also be converted back to α-ketoglutarate to replenish TCA cycle intermediates or for oxidative ATP synthesis (29) (Figure 2B). In yeast cells, this can occur during growth in non-preferred carbon sources (30). It is therefore essential to determine the relative importance of these outcomes of glutamine metabolism in *npr2*Δ cells. We noted that α-ketoglutarate amounts in *npr2*Δ cells were higher than WT cells initially, but decreased after 4.5 h (Fig. S1). In yeast cells growing in poor carbon sources (such as lactate), the Gdh2 isoform favors glutamate to α-ketoglutarate conversion, enabling glutamine and glutamate to serve as anaplerotic substrates to feed the TCA cycle (30). *npr2*Δ cells lacking Gdh2 (*gdh2*Δ/*npr2*Δ) grew as well as *npr2*Δ cells (Fig. S1). These data suggested that *npr2*Δ cells did not require glutamine-dependent anaplerosis for growth in SL medium. In contrast, continuing glutamine consumption for nitrogen would predict increased glutamine-derived metabolites, such as glutathione, NAD^+ and nucleotides (Fig. 2B). Indeed, we observed that these metabolites were substantially higher in *npr2*Δ cells (Fig. 2C, Table 1). Furthermore, while nucleoside amounts decreased in *npr2*Δ cells compared to WT cells in SL medium, nucleotides increased substantially (Fig. 2C, Table 1), consistent with *npr2*Δ cells consuming nucleosides to sustain high nucleotide synthesis required for proliferation.

Although correlative, these trends do not directly demonstrate whether *npr2*Δ cells increase ammonium assimilation to glutamine, and if *npr2*Δ cells consume more glutamine to make these nitrogenous metabolites. To address this, we utilized metabolic flux analysis with ^{15}N-labeled nitrogen sources, enabling measurements of newly synthesized ^{15}N-labeled metabolites. To measure ammonium incorporation into glutamine-derived metabolites, we switched WT and *npr2*Δ cells from YPL to SL medium containing ^{15}N-ammonium sulfate as the only nitrogen source, and measured relative amounts of ^{15}N-labeled glutathione, NAD^+ and nucleotides (IMP, AMP and GMP) (Fig. 2D, Fig. S2). The increases in molecular mass, and product and fragment ion *m*/z values detected from the ^{15}N-labeled forms of these metabolites are illustrated in Fig. S2. We observed that relative amounts of these ^{15}N-labeled metabolites increased >1,000 fold in *npr2*Δ cells compared to WT cells (Fig. 2D), which exhibited very little new synthesis of glutathione, NAD^+ and nucleotides. We simultaneously measured unlabeled (^{14}N) metabolites, enabling estimates of newly synthesized vs existing (^{15}N-labeled vs ^{14}N-labeled) pools (Fig. 2E). In contrast to WT cells, significant fractions of the total pool of these metabolites in npr2Δ cells were ^{15}N-labeled (Fig. 2E). We therefore conclude that in SL medium, *npr2*Δ cells increase ammonium assimilation to synthesize nitrogenous metabolites important for growth.

These data would predict that *npr2*Δ cells would require nucleotide synthesis for proliferation. Although most nucleotide biosynthesis enzymes are essential, precluding the use of gene knock-outs to determine specific roles in growth, yeast have two complementing isoforms of a *de novo* purine biosynthesis enzyme, Ade16 and Ade17 (31). Since deletions of either isoform individually does not affect WT cell growth (31), we compared the growth of *ade16*Δ and *ade17*Δ cells in a WT or *npr2*Δ background. *npr2*Δ/*ade16*Δ (but not *npr2*Δ/

*ade17*Δ) cells showed substantially reduced proliferation (Fig. S1), suggesting that nucleotide biosynthesis was critical for sustaining proliferation of *npr2*Δ cells.

Increased glutamine utilization as a nitrogen source in *npr2*Δ mutants

To determine if *npr2*Δ maintained high glutamine consumption for synthesis of nitrogenous metabolites, we switched WT or *npr2*Δ cells from YPL to SL medium (with ~40 mM ammonium sulfate) and supplemented them with 1 mM ^{15}N glutamine. We then measured amounts of ^{15}N labeled metabolites, targeting our analysis to those species of these metabolites where the nitrogen is directly donated by glutamine, and excluding nitrogens indirectly derived from glutamine (Fig. S2, Fig. 3A). The amounts of ^{15}N containing species for these metabolites dramatically increased in *npr2*Δ cells relative to WT cells (Fig. 3A), similar to what we had observed with labeled ammonium sulfate as the sole nitrogen source (Fig. 2D).

We next asked if *npr2*Δ cell proliferation in SL medium was dependent on glutamine consumption. The glutamate dehydrogenase enzyme isoforms Gdh1 and Gdh3 prefer converting α-ketoglutarate to glutamate, which is then converted to glutamine (Fig. 2B) (32, 33). Deletion of *GDH1* in *npr2*Δ cells almost completely blocked proliferation (Figure 3B). In contrast, in WT cells, deletion of *GDH1* had a minor effect on proliferation over a similar amount of time in SL medium (~12 h) (Fig. S3). The Gdh3 isoform had a smaller role in supporting *npr2*Δ proliferation (Fig. S3). We also observed that 0.5 mM glutamine, and not cell-permeable α-ketoglutarate, rescued proliferation of *npr2*Δ/*gdh1*Δ cells, allowing proliferation until the glutamine in the medium was depleted (Fig. 3B). Finally, Glt1 (which reconverts glutamine to glutamate) played a smaller role in *npr2*Δ proliferation (Fig. 3C). Collectively, our data show that *npr2*Δ cells are metabolically adapted to consume glutamine to synthesize nitrogenous metabolites for proliferation. Moreover, providing WT cells in SL medium with excess glutamine did not increase proliferation (Fig. S3), strongly suggesting that the ability to consume glutamine, and not glutamine availability itself, controlled cell growth under these conditions.

These data could therefore predict altered regulation of glutamine biosynthesis enzymes in *npr2*Δ cells. Yeast cells adapt extensively to nitrogen availability. In preferred nitrogen sources such as glutamine, they repress the utilization of non-preferred sources through nitrogen catabolite repression (NCR) (26, 32, 34), whereas in poor nitrogen sources, they attempt to restore glutamine amounts (26, 32, 34, 35). We observed that Gdh1 and Gln1 enzyme amounts in WT cells decreased slowly in SL medium as cells accumulated glutamine (Fig. 3D). In contrast, Gdh1 and Gln1 increased substantially in *npr2*Δ cells (Fig. 3D). Finally, we examined the regulation of the transcription factor Gln3 which is activated during nitrogen starvation (10, 34, 36). The responses of Gln3 to nitrogen sources are complex (36, 37), but in general Gln3 is hyperphosphorylated and inactive in preferred nitrogen sources, and this regulation is only in part TORC1-dependent (10, 26, 34, 36–40). We tested if Gln3 activity was distinct between WT and *npr2*Δ cells. In rich medium (YPL), Gln3 phosphorylation (as measured by a gel mobility shift assay) in WT and *npr2*Δ cells was high, and decreased upon TORC1 inhibition with rapamycin (used only as a positive control) (Fig. 3E). However, in SL medium, WT cells showed an immediate decrease in

Gln3 phosphorylation, which then became hyperphosphorylated as glutamine concentrations increased (Fig. 3E). In contrast, in *npr2*Δ cells, Gln3 remained phosphorylated in SL medium (Fig. 3E). Collectively, our data suggest that in SL medium, *npr2*Δ cells bypass normal nitrogen-sensing mechanisms and no longer recognize poor nitrogen sources, but instead grow as if present in preferred nitrogen sources, with abnormal increases in the protein amounts of glutamine biosynthesis enzymes.

Methionine promotes glutamine consumption for nitrogenous metabolite biosynthesis

We previously observed that in SL medium, WT cells were limited in their ability to synthesize sufficient sulfur-containing amino acid (SAA) metabolites (21). The sole addition of either methionine or its downstream metabolite SAM could inhibit autophagy and promote growth, suggesting that these sulfur metabolites were limiting for growth (21). We therefore wondered if in addition to glutamine, SAM amounts in *npr2*Δ cells also differed from WT cells. Indeed, we observed that *npr2*Δ cells in SL medium accumulated higher SAM and cysteine amounts compared to WT cells following switch to SL medium (Fig. 4A, Table 1). Furthermore, the addition of methionine alone dramatically increased WT cell proliferation (Fig. 4B), suggesting the possibility that methionine might promote glutamine consumption for nitrogen.

To test this hypothesis, WT cells were switched from YPL to SL medium with or without methionine, containing ^{15}N labeled ammonium sulfate as the sole nitrogen source, and amounts of ^{15}N labeled glutathione, NAD^+ and nucleotides were measured (Fig. 4C, Fig. S2). We observed that relative amounts of these metabolites substantially increased in cells growing in SL + methionine (Fig. 4C). Furthermore, a sizable fraction of the total pool of these metabolites were newly synthesized (^{15}N labeled) only in the methionine supplemented cells (Fig. 4D). Similarly, we switched WT cells to SL or SL+met medium supplemented with ^{15}N glutamine and measured ^{15}N labeled glutathione, NAD^+ and nucleotides, targeting our analysis to those species where the nitrogen is directly donated by glutamine (Fig. S4, Fig. S2). The relative amounts of ^{15}N containing species for these metabolites dramatically increased in WT cells growing with methionine supplemented (Fig. S4). Thus, the presence of methionine alone in SL medium mimicked the growth and metabolic phenotypes of *npr2*Δ cells.

We then compared the ability of methionine and glutamine to inhibit autophagy in WT versus *npr2*Δ cells under several autophagy-inducing paradigms. In WT cells, autophagy was induced in SL medium as well as in SL medium devoid of nitrogen (SL-N), as indicated by the accumulation of free GFP cleaved from *IDH1-GFP* (Fig. 4E). Such SL-induced autophagy was inhibited in WT cells by adding methionine but not glutamine (Fig. 4E). However, autophagy in SL-N medium was not inhibited by either glutamine or methionine alone (Figure 4E). In contrast, in *npr2*Δ cells autophagy occurred only in SL-N medium, which was rescued by adding glutamine alone (Fig. 4E). Moreover, we had shown that methionine inhibits autophagy in SL medium through its ability to promote the Ppm1-catalyzed methylation of PP2A (21) (Fig. 4D). Accordingly, upon testing the importance of Ppm1 for proliferation in SL medium, we found that *ppm1*Δ cells could not proliferate, while *npr2*Δ/*ppm1*Δ cells proliferated faster than WT cells, albeit slower than *npr2*Δ cells

(Fig. 4F). This suggests that the methylation of PP2A contributes significantly to the increased growth observed in *npr2*Δ mutants, which have higher SAM amounts. We conclude that the rewiring of metabolism in *npr2*Δ cells promotes growth under these conditions through synergistic effects of increased SAM, increased PP2A methylation, and increased utilization of glutamine as a nitrogen donor.

Changes in metabolism in *npr2*Δ cells depend on TORC1

Since the Npr2 complex negatively regulates TORC1 (14, 19, 20), we asked if the metabolic differences in *npr2*Δ cells were mediated by TORC1. To address this, we transferred WT and *npr2*Δ cells growing in YPL medium to SL medium containing sub-lethal concentrations of the TORC1 inhibitor rapamycin, and compared metabolite profiles (Fig. 5A, Table 2). Upon rapamycin treatment, the direction and fold changes for most metabolites measured from WT and *npr2*Δ cells were largely indistinguishable across the time course (Fig. 5A). We also compared amounts of glutamine and SAM in WT cells switched to SL medium with *npr2*Δ cells switched to SL medium + rapamycin (Fig. 5B). In the presence of rapamycin, glutamine amounts now steadily increased in *npr2*Δ cells, in a manner similar to WT cells (Fig. 5B). Furthermore, SAM amounts in *npr2*Δ cells remained similar to or lower than that of WT cells (Fig. 5B). These data suggest that most metabolic differences caused by absence of Npr2 were TORC1-dependent.

Constitutively active Gtr1 mimics the growth and metabolic phenotypes of *npr2*Δ

Since the Npr2 complex inhibits the Rag GTPase Gtr1 (19), and the GTP-bound form of Gtr1 activates TORC1 (13), we wondered how much of the metabolic and proliferative changes in *npr2*Δ were Gtr1-dependent (Fig. 6A). We compared the proliferation of *npr2*Δ cells with those overexpressing constitutively active Gtr1 (*Gtr1-Q65L*), wherein TORC1 remains activated (13, 41), in SL medium (Fig. 6A). The *Gtr1-Q65L* overexpressing, *npr2*Δ and *npr2*Δ/*Gtr1-Q65L* cells all had similar rates of proliferation (Fig. 6A).

We compared glutamine-derived metabolites between *Gtr1-Q65L* and WT cells and found that glutamine was low in *Gtr1-Q65L* cells (Fig. 6B), while NAD^+ and glutathione increased (Fig. 6C). These metabolite profiles closely resembled *npr2*Δ cells (Fig. 2). *Gtr1-Q65L* cells also recovered faster from SAM starvation compared to WT cells (Fig. S5, Fig. 4), although not as effectively as *npr2*Δ cells. Consistent with these results, in *Gtr1-Q65L* cells, there was no evidence of autophagy as assayed by cleavage of *IDH1-GFP* (Fig. S5), suggesting that these cells bypassed autophagy in SL medium just like *npr2*Δ cells. Taken together, we conclude that the metabolic and proliferative changes in *npr2*Δ cells under these conditions are Gtr1-activation dependent.

Sch9 controls proliferation in *npr2*Δ cells

TORC1 increases translation and growth by activating the ribosomal S6K (8), which in yeast is Sch9 kinase (42). We compared the proliferation rates of WT, *npr2*Δ, *sch9*Δ, and *npr2*Δ/*sch9*Δ cells (Fig. 7A) and noted that *npr2*Δ/*sch9*Δ cells were unable to proliferate in SL medium (Fig. 7A), indicating that Sch9 was essential for the proliferation of *npr2*Δ cells. Additionally, *sch9*Δ cells proliferated slower than WT cells, suggesting that basal TORC1 activity was required in WT cells in SL medium.

Since TORC1-dependent phosphorylation is critical for Sch9 activity (42), we tested if Sch9 phosphorylation differed between WT and *npr2*Δ cells in SL medium. Because Sch9 has an apparent SDS-PAGE gel mobility of >100 kDa, a chemical cleavage assay yielding a ~35 kDa carboxy terminal fragment containing the major Sch9 phosphorylation sites is the standard assay used to measure Sch9 phosphorylation (42). The phosphorylated form of this fragment indicates TORC1 activity and exhibits decreased SDS-PAGE mobility (42). Using this assay, we noted decreased Sch9 mobility in both WT and *npr2*Δ cells in rich medium, which was reversed upon the addition of rapamycin (Figure 7B), as has been observed previously (19). In SL medium however, we observed increased Sch9 Western blot signal intensity over time only in *npr2*Δ and not WT cells (Fig. 7B). Additionally, the decreased mobility of Sch9 in *npr2*Δ cells grown in SL medium was less than in rich media (Fig. 7B).

This increased Sch9 blot intensity in *npr2*Δ cells with a modest mobility shift in SL medium was puzzling. Since Sch9 transcripts remained constant in WT and *npr2*Δ cells (Fig. 7C), and blots were normalized for total protein (Fig. 7B), this increased signal was unlikely due to increased Sch9 protein. However, since Sch9 is epitope tagged (3X HA) at the C-terminus, we wondered if the HA antibody preferred recognition of the phosphorylated form of Sch9-3XHA. If so, the signal detected for the phosphorylated form of Sch9 would be greater than the dephosphorylated version, for the same amount of protein. Indeed, when Sch9-3xHA tagged cells were lysed in the absence of protein phosphatase inhibitors, anti-HA blots showed decreased signal intensity (Fig. 7D). Additionally, when immunoprecipitated Sch9-3xHA was treated with λ-phosphatase, the Western blot signal intensity was substantially reduced (Fig. 7D). This effect was likely more pronounced when detecting only the C-terminal fragment of Sch9 (Fig. 7B). We conclude that the increased Sch9 signal observed in *npr2*Δ cells compared to WT cells in SL medium (Fig. 7B) is indeed due to increased Sch9 phosphorylation and thus TORC1 activity. These data caution that the apparent levels of Sch9 phosphorylation must be interpreted carefully especially under non-fermentable carbon sources.

Discussion

As a key regulator of metabolism, the TORC1 pathway balances cell growth with survival (43), yet TORC1-regulated metabolic transformations driving cell proliferation are not well understood. Herein, we have defined a metabolic and mechanistic basis of how the Npr2 complex, through TORC1, regulates cell growth in a challenging non-fermentable carbon source (lactate). The loss of Npr2 results in a “hyperproliferative” metabolic state (Fig. 1), switching from glutamine accumulation to consumption, thereby supplying cells with nitrogenous metabolites required for proliferation (Fig. 2, 3). Concomitantly, these cells have increased SAM (Fig. 4), which can drive cell growth and proliferation through the action of Ppm1/methylated PP2A (21), and increased tRNA thiolation (44). Our data are consistent with a model wherein the loss of Npr2 disrupts the Npr2 complex, relieving Gtr1 inhibition and activating TORC1 (Fig. 7E). This TORC1 activation alters both nitrogen and sulfur metabolism to provide building-blocks for proliferation (Fig. 7E), and the SAM-dependent regulation of PP2A methylation drives a feed-forward loop further activating TORC1 and promoting growth. A striking observation from our studies is that in WT cells growing in amino acid-free lactate medium, methionine supplementation promotes nitrogen

assimilation and consumption of glutamine for nitrogen, recapitulating the metabolic and proliferative phenotypes observed in *npr2*Δ cells (Fig. 4). This regulation of nitrogen and sulfur amino acid metabolism appears to be critical for switching between proliferation and autophagy.

Our studies reveal that the role of the Npr2 complex in regulating nitrogen metabolism, glutamine utilization and TORC1 activity depends upon nutritional context, including the carbon source used by the cells. Previous studies of the yeast Npr2 complex and TORC1, are limited to rich glucose-containing medium (14, 15, 19, 45). Under these conditions, *npr2*Δ cells are maladapted to environments where the nitrogen source quality is poor (e.g., ammonium) (14), but grow normally in the presence of the preferred nitrogen source glutamine (14). Our investigations were performed under a more-challenging, non-fermentable carbon source (lactate), and not glucose. It should be noted that Npr2 is degraded by the F-box ubiquitin ligase Grr1 (Glucose repression resistant 1) (15). Grr1 functions primarily in carbon catabolite repression (46, 47), and has marginal roles in non-fermentable carbon sources, suggesting that the function of Npr2 becomes more important to the cell upon glucose depletion. We provide important insights into how the Npr2 complex regulates nitrogen consumption and growth under conditions that demand oxidative metabolism. Under these conditions, the Npr2 complex controls nitrogen preference, and its absence mimics nitrogen catabolite repression leading to increased nitrogen consumption and unchecked growth. These diverse observations indicate distinct roles and modes of regulation for Npr2 depending upon the nature of the carbon source. Nonetheless, a consensus model emerges in which the Npr2 complex functions to inactivate TORC1 as means to slow down glutamine utilization and promote its accumulation. Loss of Npr2 function in glucose + ammonium medium may promote glutamine synthesis and utilization at the expense of other metabolic processes, thus leading to slower growth.

There is considerable interest in the interplay between TORC1 and glutamine in growth regulation. Glutamine in conjunction with leucine is thought to activate TORC1 by increasing leucine transport (48); or glutaminolysis, although the precise mechanisms remain unclear (45, 49–51). We show that in glucose-deficient minimal conditions, TORC1 activation through the loss of *npr2*Δ increases glutamine metabolism to synthesize nitrogen-containing metabolites, despite lower intracellular leucine (Fig. 2). Furthermore, supplementing glutamine neither increased TORC1 activity, nor proliferation in WT cells (Fig. 7, Fig. S3). As such, glutamine metabolism instead appears to be downstream of the Npr2 complex-Gtr1-TORC1 during such nutrient limitations. We propose a central function of TORC1 in increasing the synthesis and utilization of glutamine as a nitrogen donor for biosynthesis, with a key role of the Npr2-complex in modulating TORC1 activity according to the cell's needs. Finally, while studies of cancer cell lines have focused on the utilization of glutamine as a carbon source (29, 52, 53), our results reiterate the importance of glutamine as a nitrogen source for biosynthesis of numerous important metabolites, including amino acids, nucleotides, glutathione, and NAD^+ (32, 34, 35, 54) that fuel cell proliferation. Lack of Npr2 function in certain nutritional contexts may therefore cause dysregulations in metabolism that could promote transformation.

Materials and Methods

Yeast strains, gene deletion, tagging and mutagenesis

The prototrophic CEN.PK strain background was used in all experiments. Strains used in this study are listed in the Supplementary Table S1. Gene deletions or tagging was performed using a PCR based strategy as described (55).

Generation of the *GTR1-Q65L* strain

The GTR1 CDS and TEF1 promoter for overexpression were amplified and inserted into the *Sma*I site in *HO*-poly-HygroMX4-*HO* plasmid (56). The *HO*-TEF1p-GTR1 Q65L-HygroMX4-*HO* plasmid was subsequently made by Site-Directed Mutagenesis, and these constructs were stably expressed at the HO locus in WT yeast.

Media composition

Standard formulations for rich medium (yeast extract, peptone) or synthetic minimal medium (YNB and ammonium sulfate without amino acids), with 2% concentrations of the specified carbon source were used. Supplemented amino acids: Methionine, glutamine, α-ketoglutarate (dimethyl-alpha-KG) 0.5 mM each, Non-S mixture contains 1 mM each amino acid (except Met, Cys, Tyr) or as specified in the text.

Cell growth in different media

Unless specified, cells were grown in rich medium with lactate as the carbon source (YPL) for ~36 h with repeated dilutions, in order to acclimatize cells to growth in lactate, and were subsequently switched to YPL, minimal medium with lactate (SL), or as indicated. Cell proliferation curves in different media used cultures started at OD_{600} ~0.15–0.2.

RNA purifications and RT-qPCR

Total RNA from yeast cells was isolated using a MasterPure Yeast RNA kit (Epicentre). Reverse transcription was performed on 1 μg of purified total RNA, using SuperScript-II reverse transcriptase (Invitrogen). Quantitative PCR was performed using SYBR® Green, validated primers, template cDNA, and transcript abundance normalized to ACT1.

Cell collection, protein extraction and detection

Equal numbers of cells were collected from respective cultures,flash-frozen in liquid nitrogen, and lysed in 50mM NaCl, 100mM Tris pH 7.5, 1mM EDTA, 1mM EGTA, 10% glycerol, 0.5% Triton X-100, 2 mM β-mercaptoethanol, protease inhibitors, and phosphatase inhibitors (50mM Sodium Fluoride, 2mM Sodium Orthovanadate), by bead-beating using glass beads. Protein concentrations from extracts measured using a BCA assay. Equal amounts of samples were resolved on 12% or 4–12% Bis-Tris gels, and detected as specified. Coomassie-blue stained gels or western blots for G6PD were used as loading controls.

Antibodies used

monoclonal anti-flag M2, anti-G6PD (Sigma); anti-HA 12CA5, anti-GFP (Roche).

Detection of phosphorylated Sch9 using NTCB cleavage

The Sch9 gel mobility shift assay was modified from (42). ~10 OD cells in culture were rapidly harvested by centrifugation after quenching in 10% TCA, pellets were flash frozen, and cells lysed in 300 μl buffer containing 50 mM Tris [pH 7.5], 5 mM EDTA, 6 M urea, 1% SDS, 1mMPMSF, and protein phosphatase inhibitors (50mM sodium fluoride, 2mM sodium orthovanadate) by bead-beating with glass beads, with sub- sequent heating (10 min/65° C). Lysates were collected after centrifugation and protein concentrations were measured, normalized. The NTCB cleavage assay was performed as described (42). Further analysis was done by SDS-PAGE separation and immunoblotting using anti-HA antibody.

Cells for metabolite extractions

Cells were grown in YPL medium for ~36 h with repeated dilutions, diluted in YPL (OD 0.01), and grown to an OD_{600} of ~1.0 and collected for metabolite extractions, or rapidly harvested, and transferred to minimal lactate (SL) medium, and collected for metabolite extractions at specified times. Metabolites were extracted as described earlier in 75% ethanol (44, 57). Acidic extractions (to preserve oxidation sensitive metabolites) were done in 75% ethanol with 0.1% formic acid.

Metabolite analysis by LC-MS/MS

Extracted metabolites were measured using targeted LC-MS/MS methods, expanding methods described previously (44, 57). A library of common metabolites was constructed using standards, and metabolites were detected using an Applied Biosystems 3200 QTRAP triple quadrupole-linear ion trap mass spectrometer for quantitative optimization detection of daughter ions upon collision-induced fragmentation of the parent ion [multiple reaction monitoring (MRM)]. For each metabolite, parameters for quantitation of the two most abundant daughter ions (i.e., two MRMs per metabolite) were included. Metabolites were separated chromatographically using a Synergi Fusion column (150 ´2.0 mm 4 m, Phenomenex), using a Shimadzu Prominence LC20/SIL-20AC HPLC-autosampler coupled to the mass spectrometer. Buffers for positive mode analysis: Buffer A: 99.9% H_2O/0.1% formic acid, Buffer B: 99.9% methanol /0.1% formic acid. *T* = 0 min, 0% B; *T* = 4 min, 0% B; *T* = 11 min, 50% B; *T* = 13 min, 100% B; *T* = 15 min, 100% B, *T* = 16 min, 0% B; *T* = 20 min, stop, or Buffer A: 5 mM ammonium acetate in H_2O, Buffer B: 5 mM ammonium acetate in 100% methanol. Buffers for negative mode analysis: 5 mM TBA (Buffer A), and 100% methanol (Buffer B). The area under each peak was quantitated by using Analyst software, inspected for accuracy, and normalized against total ion count, following which relative amounts were measured, setting metabolite amounts from WT samples in the first time point to 1.

^{15}N ammonium sulfate or glutamine labeling and metabolic flux analysis

^{15}N labeled ammonium sulfate ($(^{15}NH_4)_2SO_4$) or glutamine ($H_2{}^{15}NCOCH_2CH_2CH(^{15}NH_2)CO_2H$) were obtained from Cambridge Isotope Laboratories, Inc. Cells were grown in YPL, and switched to SL medium where all the ammonium sulfate (sole nitrogen source) was ^{15}N labeled, or SL medium was supplemented with 1 mM ^{15}N glutamine, and cells were collected, metabolites extracted as described earlier. ^{15}N labeled

metabolites were detected by LC-MS/MS, with the targeted parent and daughter ions specific to the ^{15}N form of the metabolites, as illustrated in Fig. S2.

Hierarchical clustering analysis and heat maps

For hierarchical clustering analysis normalized metabolite amounts were log_2-transformed, centered about the mean, normalized, and clustered by Spearman–Rank correlation using the Cluster software (58, 59), and the data visualized as heat-maps built using Java Treeview.

Measurement of autophagy

Autophagy was measured using an Idh1-GFP cleavage assay, as described earlier (18, 21). The accumulation/presence of cleaved GFP was used as an indicator of autophagy.

Supplementary Material

Refer to Web version on PubMed Central for supplementary material.

Acknowledgements

This work was funded by NIH grant R01GM094314 and the Welch Foundation (I-1797) to B.P.T.

References and Notes

1. Rabinowitz JD, White E. Autophagy and metabolism. Science. 2010; 330:1344–1348. [PubMed: 21127245]
2. Yuan HX, Xiong Y, Guan KL. Nutrient sensing, metabolism, and cell growth control. Molecular cell. 2013; 49:379–387. [PubMed: 23395268]
3. Hanahan D, Weinberg RA. Hallmarks of cancer: the next generation. Cell. 2011; 144:646–674. [PubMed: 21376230]
4. Deberardinis RJ, Sayed N, Ditsworth D, Thompson CB. Brick by brick: metabolism and tumor cell growth. Current opinion in genetics & development. 2008; 18:54–61. [PubMed: 18387799]
5. DeBerardinis RJ, Lum JJ, Hatzivassiliou G, Thompson CB. The biology of cancer: metabolic reprogramming fuels cell growth and proliferation. Cell metabolism. 2008; 7:11–20. [PubMed: 18177721]
6. Wullschleger S, Loewith R, Hall MN. TOR signaling in growth and metabolism. Cell. 2006; 124:471–484. [PubMed: 16469695]
7. Loewith R, Hall MN. Target of rapamycin (TOR) in nutrient signaling and growth control. Genetics. 2011; 189:1177–1201. [PubMed: 22174183]
8. Ma XM, Blenis J. Molecular mechanisms of mTOR-mediated translational control. Nature reviews. Molecular cell biology. 2009; 10:307–318.
9. Jewell JL, Russell RC, Guan KL. Amino acid signalling upstream of mTOR. Nature reviews. Molecular cell biology. 2013; 14:133–139.
10. Broach JR. Nutritional control of growth and development in yeast. Genetics. 2012; 192:73–105. [PubMed: 22964838]
11. Sancak Y, Bar-Peled L, Zoncu R, Markhard AL, Nada S, Sabatini DM. Ragulator-Rag complex targets mTORC1 to the lysosomal surface and is necessary for its activation by amino acids. Cell. 2010; 141:290–303. [PubMed: 20381137]
12. Kim E, Goraksha-Hicks P, Li L, Neufeld TP, Guan KL. Regulation of TORC1 by Rag GTPases in nutrient response. Nature cell biology. 2008; 10:935–945.
13. Binda M, Peli-Gulli MP, Bonfils G, Panchaud N, Urban J, Sturgill TW, Loewith R, De Virgilio C. The Vam6 GEF controls TORC1 by activating the EGO complex. Molecular cell. 2009; 35:563–573. [PubMed: 19748353]

14. Neklesa TK, Davis RW. A genome-wide screen for regulators of TORC1 in response to amino acid starvation reveals a conserved Npr2/3 complex. PLoS genetics. 2009; 5:e1000515. [PubMed: 19521502]
15. Spielewoy N, Guaderrama M, Wohlschlegel JA, Ashe M, Yates JR 3rd, Wittenberg C. Npr2, yeast homolog of the human tumor suppressor NPRL2, is a target of Grr1 required for adaptation to growth on diverse nitrogen sources. Eukaryotic cell. 2010; 9:592–601. [PubMed: 20154027]
16. Rousselet G, Simon M, Ripoche P, Buhler JM. A second nitrogen permease regulator in Saccharomyces cerevisiae. FEBS letters. 1995; 359:215–219. [PubMed: 7867803]
17. Dokudovskaya S, Waharte F, Schlessinger A, Pieper U, Devos DP, Cristea IM, Williams R, Salamero J, Chait BT, Sali A, Field MC, Rout MP, Dargemont C. A conserved coatomer-related complex containing Sec13 and Seh1 dynamically associates with the vacuole in Saccharomyces cerevisiae. Molecular & cellular proteomics : MCP. 2011; 10 M110 006478.
18. Wu X, Tu BP. Selective regulation of autophagy by the Iml1-Npr2-Npr3 complex in the absence of nitrogen starvation. Molecular biology of the cell. 2011; 22:4124–4133. [PubMed: 21900499]
19. Panchaud N, Peli-Gulli MP, De Virgilio C. Amino acid deprivation inhibits TORC1 through a GTPase-activating protein complex for the Rag family GTPase Gtr1. Science signaling. 2013; 6:ra42. [PubMed: 23716719]
20. Bar-Peled L, Chantranupong L, Cherniack AD, Chen WW, Ottina KA, Grabiner BC, Spear ED, Carter SL, Meyerson M, Sabatini DM. A Tumor suppressor complex with GAP activity for the Rag GTPases that signal amino acid sufficiency to mTORC1. Science. 2013; 340:1100–1106. [PubMed: 23723238]
21. Sutter BM, Wu X, Laxman S, Tu BP. Methionine Inhibits Autophagy and Promotes Growth by Inducing the SAM-Responsive Methylation of PP2A. Cell. 2013; 154:403–415. [PubMed: 23870128]
22. Li J, Wang F, Haraldson K, Protopopov A, Duh FM, Geil L, Kuzmin I, Minna JD, Stanbridge E, Braga E, Kashuba VI, Klein G, Lerman MI, Zabarovsky ER. Functional characterization of the candidate tumor suppressor gene NPRL2/G21 located in 3p21.3C. Cancer research. 2004; 64:6438–6443. [PubMed: 15374952]
23. Zabarovsky ER, Lerman MI, Minna JD. Tumor suppressor genes on chromosome 3p involved in the pathogenesis of lung and other cancers. Oncogene. 2002; 21:6915–6935. [PubMed: 12362274]
24. Schenk PW, Brok M, Boersma AW, Brandsma JA, Den Dulk H, Burger H, Stoter G, Brouwer J, Nooter K. Anticancer drug resistance induced by disruption of the Saccharomyces cerevisiae NPR2 gene: a novel component involved in cisplatin- and doxorubicin-provoked cell kill. Molecular pharmacology. 2003; 64:259–268. [PubMed: 12869630]
25. Sancak Y, Peterson TR, Shaul YD, Lindquist RA, Thoreen CC, Bar-Peled L, Sabatini DM. The Rag GTPases bind raptor and mediate amino acid signaling to mTORC1. Science. 2008; 320:1496–1501. [PubMed: 18497260]
26. Ljungdahl PO, Daignan-Fornier B. Regulation of amino acid, nucleotide, and phosphate metabolism in Saccharomyces cerevisiae. Genetics. 2012; 190:885–929. [PubMed: 22419079]
27. Estrela JM, Ortega A, Obrador E. Glutathione in cancer biology and therapy. Critical reviews in clinical laboratory sciences. 2006; 43:143–181. [PubMed: 16517421]
28. Bieganowski P, Pace HC, Brenner C. Eukaryotic NAD+ synthetase Qns1 contains an essential, obligate intramolecular thiol glutamine amidotransferase domain related to nitrilase. The Journal of biological chemistry. 2003; 278:33049–33055. [PubMed: 12771147]
29. DeBerardinis RJ, Cheng T. Q's next: the diverse functions of glutamine in metabolism, cell biology and cancer. Oncogene. 2010; 29:313–324. [PubMed: 19881548]
30. Coschigano PW, Miller SM, Magasanik B. Physiological and genetic analysis of the carbon regulation of the NAD-dependent glutamate dehydrogenase of Saccharomyces cerevisiae. Molecular and cellular biology. 1991; 11:4455–4465. [PubMed: 1652057]
31. Tibbetts AS, Appling DR. Characterization of two 5-aminoimidazole-4-carboxamide ribonucleotide transformylase/inosine monophosphate cyclohydrolase isozymes from Saccharomyces cerevisiae. The Journal of biological chemistry. 2000; 275:20920–20927. [PubMed: 10877846]

32. Magasanik B. Ammonia assimilation by Saccharomyces cerevisiae. Eukaryotic cell. 2003; 2:827–829. [PubMed: 14555464]
33. DeLuna A, Avendano A, Riego L, Gonzalez A. NADP-glutamate dehydrogenase isoenzymes of Saccharomyces cerevisiae. Purification, kinetic properties, and physiological roles. The Journal of biological chemistry. 2001; 276:43775–43783. [PubMed: 11562373]
34. Cooper, TG. Nitrogen metabolism in *Saccharomyces cerevisiae*. In: Strathern, JN.; Jones, EW.; Broach, JR., editors. The Molecular Biology of the Yeast *Saccharomyces*: Metabolism and Gene Expression. Cold Spring Harbor, NY: Cold Spring Harbor Laboratory Press; 1982. p. 39-99.
35. Magasanik B, Kaiser CA. Nitrogen regulation in Saccharomyces cerevisiae. Gene. 2002; 290:1–18. [PubMed: 12062797]
36. Cooper TG. Transmitting the signal of excess nitrogen in Saccharomyces cerevisiae from the Tor proteins to the GATA factors: connecting the dots. FEMS microbiology reviews. 2002; 26:223–238. [PubMed: 12165425]
37. Tate JJ, Cooper TG. Five conditions commonly used to down-regulate tor complex 1 generate different physiological situations exhibiting distinct requirements and outcomes. The Journal of biological chemistry. 2013; 288:27243–27262. [PubMed: 23935103]
38. Beck T, Hall MN. The TOR signalling pathway controls nuclear localization of nutrient-regulated transcription factors. Nature. 1999; 402:689–692. [PubMed: 10604478]
39. Tate JJ, Rai R, Cooper TG. Ammonia-specific regulation of Gln3 localization in Saccharomyces cerevisiae by protein kinase Npr1. The Journal of biological chemistry. 2006; 281:28460–28469. [PubMed: 16864577]
40. Tate JJ, Cooper TG. Stress-responsive Gln3 localization in Saccharomyces cerevisiae is separable from and can overwhelm nitrogen source regulation. The Journal of biological chemistry. 2007; 282:18467–18480. [PubMed: 17439949]
41. Nakashima N, Noguchi E, Nishimoto T. Saccharomyces cerevisiae putative G protein, Gtr1p, which forms complexes with itself and a novel protein designated as Gtr2p, negatively regulates the Ran/Gsp1p G protein cycle through Gtr2p. Genetics. 1999; 152:853–867. [PubMed: 10388807]
42. Urban J, Soulard A, Huber A, Lippman S, Mukhopadhyay D, Deloche O, Wanke V, Anrather D, Ammerer G, Riezman H, Broach JR, De Virgilio C, Hall MN, Loewith R. Sch9 is a major target of TORC1 in Saccharomyces cerevisiae. Molecular cell. 2007; 26:663–674. [PubMed: 17560372]
43. Cornu M, Albert V, Hall MN. mTOR in aging, metabolism, and cancer. Current opinion in genetics & development. 2013; 23:53–62. [PubMed: 23317514]
44. Laxman S, Sutter BM, Wu X, Kumar S, Guo X, Trudgian DC, Mirzaei H, Tu BP. Sulfur Amino Acids Regulate Translational Capacity and Metabolic Homeostasis through Modulation of tRNA Thiolation. Cell. 2013; 154:416–429. [PubMed: 23870129]
45. Stracka D, Jozefczuk S, Rudroff F, Sauer U, Hall MN. Nitrogen Source Activates TOR (Target of Rapamycin) Complex 1 via Glutamine and Independently of Gtr/Rag Proteins. The Journal of biological chemistry. 2014; 289:25010–25020. [PubMed: 25063813]
46. Flick JS, Johnston M. GRR1 of Saccharomyces cerevisiae is required for glucose repression and encodes a protein with leucine-rich repeats. Molecular and cellular biology. 1991; 11:5101–5112. [PubMed: 1922034]
47. Johnston M, Flick JS, Pexton T. Multiple mechanisms provide rapid and stringent glucose repression of GAL gene expression in Saccharomyces cerevisiae. Molecular and cellular biology. 1994; 14:3834–3841. [PubMed: 8196626]
48. Nicklin P, Bergman P, Zhang B, Triantafellow E, Wang H, Nyfeler B, Yang H, Hild M, Kung C, Wilson C, Myer VE, MacKeigan JP, Porter JA, Wang YK, Cantley LC, Finan PM, Murphy LO. Bidirectional transport of amino acids regulates mTOR and autophagy. Cell. 2009; 136:521–534. [PubMed: 19203585]
49. Duran RV, Oppliger W, Robitaille AM, Heiserich L, Skendaj R, Gottlieb E, Hall MN. Glutaminolysis activates Rag-mTORC1 signaling. Molecular cell. 2012; 47:349–358. [PubMed: 22749528]
50. Kim SG, Hoffman GR, Poulogiannis G, Buel GR, Jang YJ, Lee KW, Kim BY, Erikson RL, Cantley LC, Choo AY, Blenis J. Metabolic stress controls mTORC1 lysosomal localization and

dimerization by regulating the TTT-RUVBL1/2 complex. Molecular cell. 2013; 49:172–185. [PubMed: 23142078]

51. Csibi A, Fendt SM, Li C, Poulogiannis G, Choo AY, Chapski DJ, Jeong SM, Dempsey JM, Parkhitko A, Morrison T, Henske EP, Haigis MC, Cantley LC, Stephanopoulos G, Yu J, Blenis J. The mTORC1 pathway stimulates glutamine metabolism and cell proliferation by repressing SIRT4. Cell. 2013; 153:840–854. [PubMed: 23663782]
52. DeBerardinis RJ, Mancuso A, Daikhin E, Nissim I, Yudkoff M, Wehrli S, Thompson CB. Beyond aerobic glycolysis: transformed cells can engage in glutamine metabolism that exceeds the requirement for protein and nucleotide synthesis. Proceedings of the National Academy of Sciences of the United States of America. 2007; 104:19345–19350. [PubMed: 18032601]
53. Mullen AR, Wheaton WW, Jin ES, Chen PH, Sullivan LB, Cheng T, Yang Y, Linehan WM, Chandel NS, DeBerardinis RJ. Reductive carboxylation supports growth in tumour cells with defective mitochondria. Nature. 2012; 481:385–388. [PubMed: 22101431]
54. Medina MA. Glutamine and cancer. The Journal of nutrition. 2001; 131:2539S–2542S. discussion 2550S-2531S. [PubMed: 11533309]
55. Longtine MS, McKenzie A 3rd, Demarini DJ, Shah NG, Wach A, Brachat A, Philippsen P, Pringle JR. Additional modules for versatile and economical PCR-based gene deletion and modification in Saccharomyces cerevisiae. Yeast. 1998; 14:953–961. [PubMed: 9717241]
56. Voth WP, Richards JD, Shaw JM, Stillman DJ. Yeast vectors for integration at the HO locus. Nucleic acids research. 2001; 29 E59-59.
57. Tu BP, Mohler RE, Liu JC, Dombek KM, Young ET, Synovec RE, McKnight SL. Cyclic changes in metabolic state during the life of a yeast cell. Proceedings of the National Academy of Sciences of the United States of America. 2007; 104:16886–16891. [PubMed: 17940006]
58. Eisen MB, Spellman PT, Brown PO, Botstein D. Cluster analysis and display of genome-wide expression patterns. Proceedings of the National Academy of Sciences of the United States of America. 1998; 95:14863–14868. [PubMed: 9843981]
59. de Hoon MJ, Imoto S, Nolan J, Miyano S. Open source clustering software. Bioinformatics. 2004; 20:1453–1454. [PubMed: 14871861]

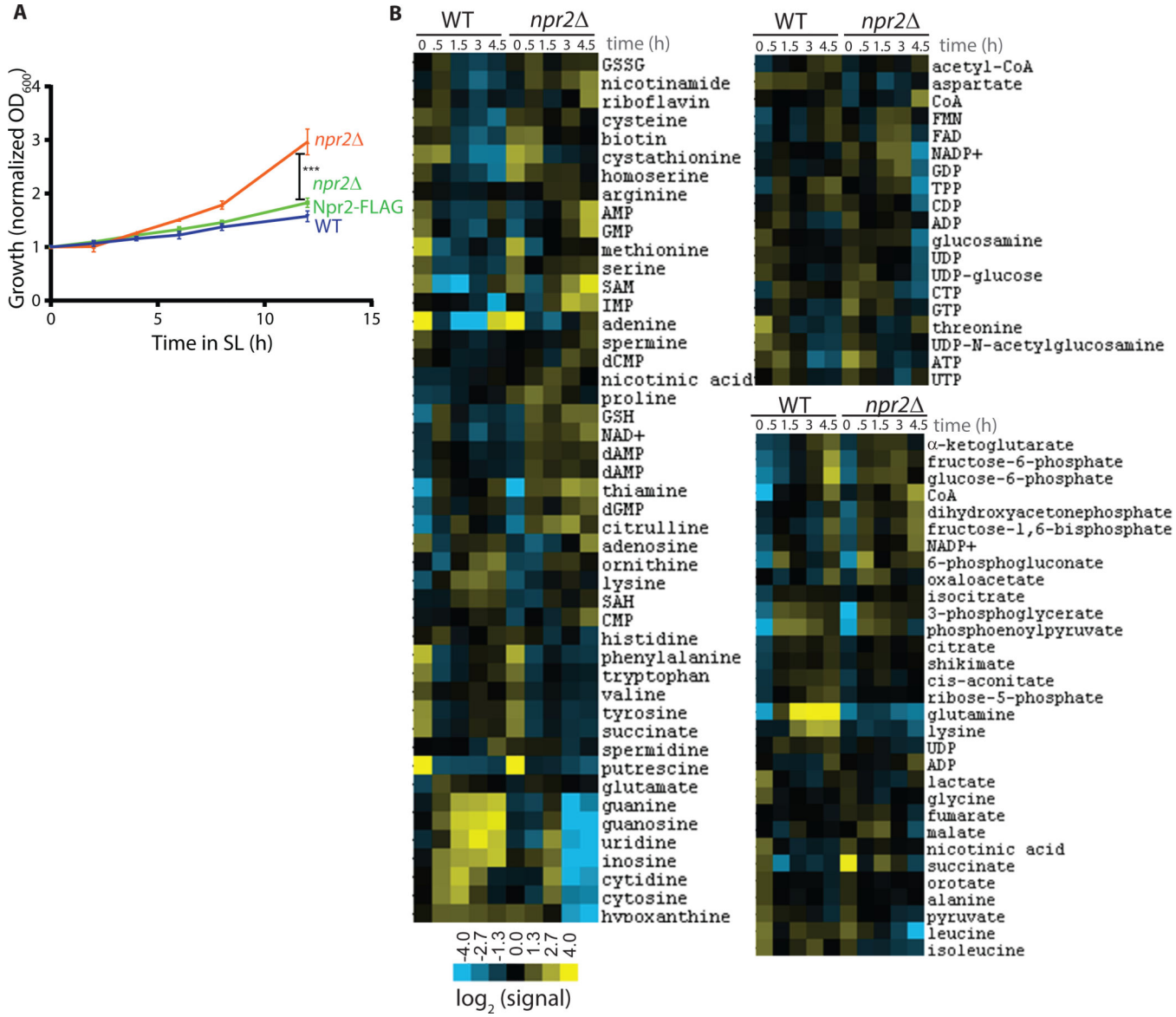

Figure 1. WT and *npr2*Δ cells have diametrically opposed metabolic states

A) An illustration of the nutrient shift that induces autophagy in WT but not *npr2*Δ cells. Cells growing in log phase in rich medium with lactate as a carbon source were harvested, and switched to minimal medium with lactate as a carbon source (SL) at the same cell density (18, 21).

B) WT, *npr2*Δ and *npr2*Δ/*NPR2-flag* cells growing in log phase in rich medium (YPL) were diluted into minimal medium (SL), and cell proliferation was measured.. n=3, mean±SD, *** p<0.001.C) (Top) Experimental strategy used for metabolite extract preparation and metabolomic analysis by LC-MS/MS. WT and *npr2*Δ cells were grown in YPL and transferred to SL medium to induce autophagy (as in panel A), after which metabolites were extracted at the indicated time points. Shown are heat-maps of hierarchical clustering analyses of metabolite profiles obtained from LC-MS/MS analysis depicting changes in intracellular metabolite amounts over time in WT and *npr2*Δ cells as measured using

multiple targeted LC-MS/MS based methods. Rows correspond to metabolites, and columns to the time points as illustrated in the schematic for either the WT or *npr2*Δ cells. Metabolite data were $\log_2$-transformed, centered about the mean, normalized, and clustered by using Spearman–Rank correlation.

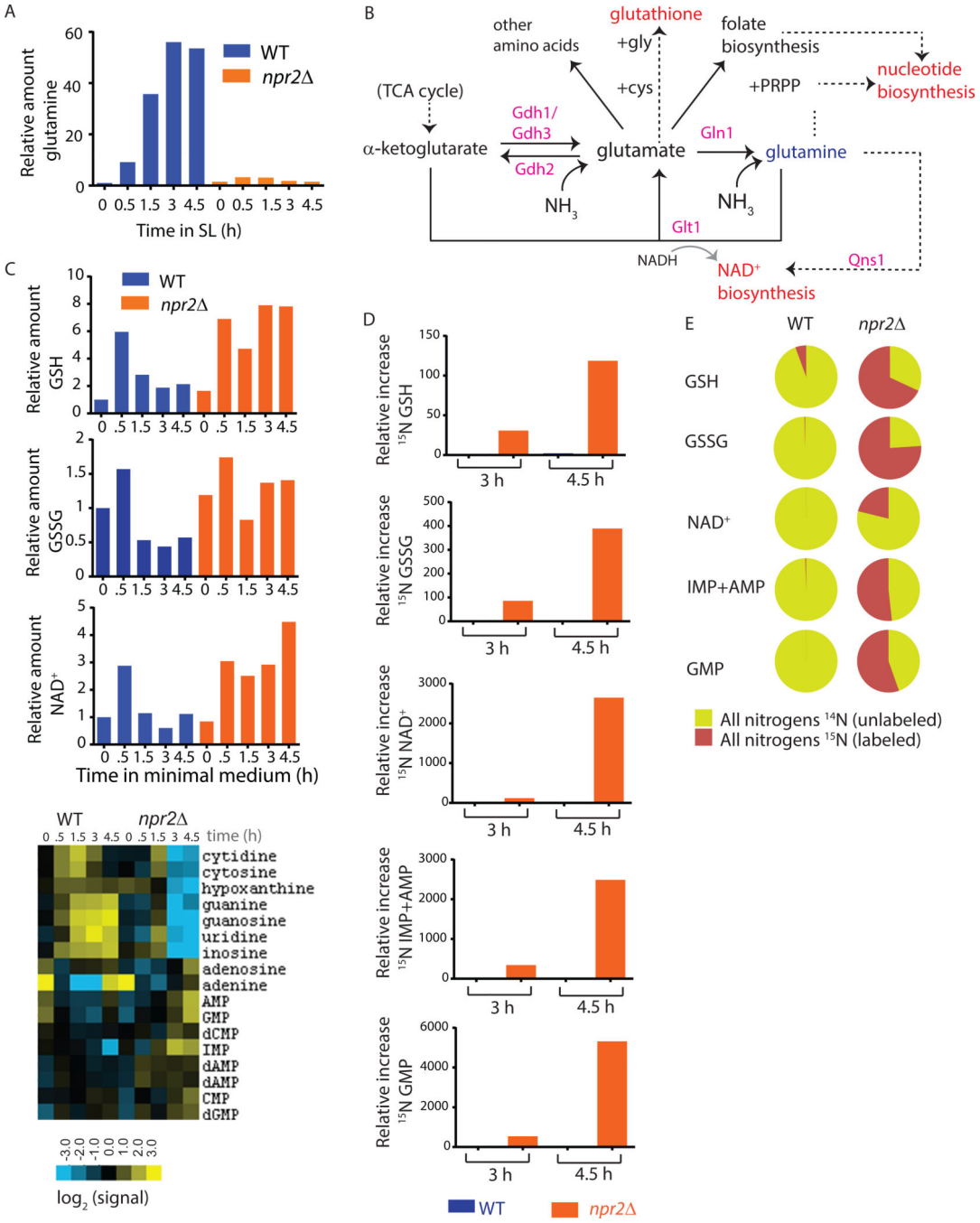

Figure 2. *npr2*Δ cells increase utilization of glutamine as a nitrogen donor for biosynthesis

A) WT but not *npr2*Δ cells induce autophagy and accumulate glutamine in SL medium. The graphs show relative intracellular glutamine amounts in WT and *npr2*Δ cells switched to minimal lactate (SL) medium, collected over 4.5 h.

B) Metabolites derived from glutamine metabolism. Glutamine can serve as a nitrogen donor for nucleotides, glutathione, de novo NAD^+ synthesis regeneration, or replenish TCA cycle intermediates through anaplerosis.

C) Nitrogenous metabolites dependent on glutamine for synthesis increase in *npr2*Δ cells. The graphs show relative amounts of reduced glutathione (GSH), oxidized glutathione (GSSG) and NAD^+ in WT and *npr2*Δ cells.

D) Ammonium incorporation into glutamine derived nitrogenous metabolites increases in *npr2*Δ cells. WT and *npr2*Δ cells were switched from YPL to SL medium containing ^{15}N ammonium sulfate as the nitrogen source, and relative changes in ^{15}N glutathione, NAD^+ and nucleotides were measured from cells collected at the specified times using LC-MS/MS as shown in the schematic on the right (also see Supplemental Figure 3 and Materials and Methods). Changes in 15N labeled metabolites are relative to WT cells 3 h after switching to SL medium.

E) Fractions of the specific nitrogenous metabolites with all nitrogens unlabeled (^{14}N), or ^{15}N labeled (newly synthesized) in WT and *npr2*Δ cells 4.5 h after switching to SL medium with ^{15}N ammonium sulfate as the sole nitrogen source.

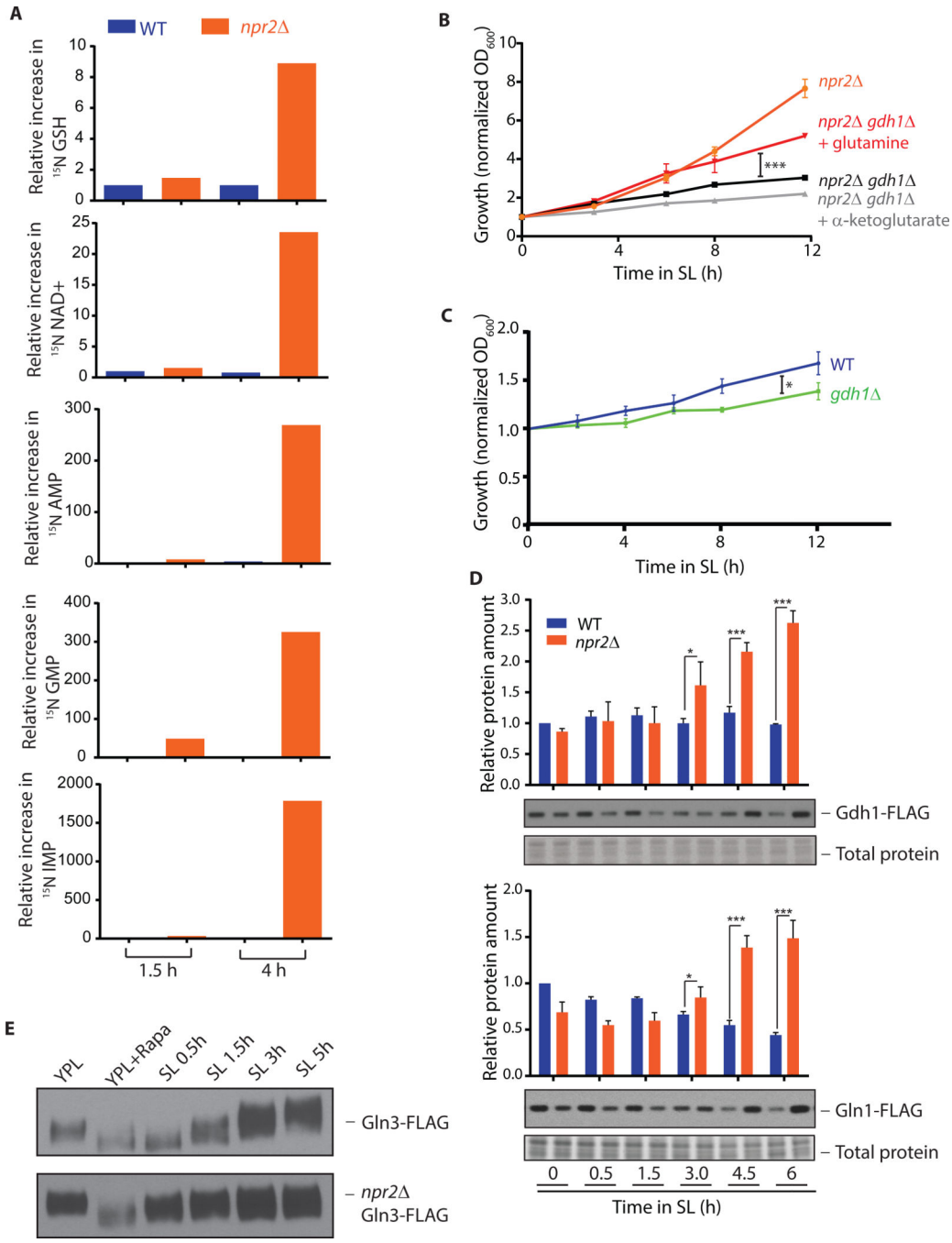

Figure 3. Glutamine is utilized as a nitrogen donor to support proliferation of *npr2Δ* cells in SL medium

A) Direct glutamine consumption for nitrogenous metabolite biosynthesis increases in *npr2*Δ cells. WT and *npr2*Δ cells were switched from YPL to SL medium supplemented with 1 mM ^{15}N glutamine, and relative changes in ^{15}N glutathione, NAD^{+} and nucleotides were measured from cells collected at the specified times using LC-MS/MS as shown in the schematic on the right (also see Supplemental Figure 3 and Materials and Methods for more details). The changes in ^{15}N labeled metabolites are relative to amounts of these metabolites in WT cells 3 h after switching to SL medium.

B) Glutamine consumption for nitrogen, and not glutaminolysis, is essential for growth in *npr2*Δ cells. WT and *npr2*Δ cell proliferation in the presence or absence of the glutamate dehydrogenase enzyme Gdh1 was measured. *npr2*Δ*/gdh1*Δ cells show reduced proliferation compared to *npr2*Δ cells. Cell growth upon addition of 0.5 mM glutamine, or α-ketoglutarate (cell permeable ester) was also measured. Note that only glutamine, and not α-ketoglutarate addition rescues growth in *npr2*Δ*/gdh1*Δ cells. n=3, mean±SD, *** $p<0.001$.
C) The role of glutamate synthase Glt1 in *npr2*Δ cell proliferation was determined by comparing the proliferation of *npr2*Δ/*glt1*Δ cells with *npr2*Δ cells. Glt1 had a relatively small role in *npr2*Δ cell proliferation. n=3, mean±SD.
D) Glutamine biosynthesis enzymes increase in *npr2*Δ cells in SL medium. Protein amounts of *GDH1-flag* or *GLN1-flag* in WT and *npr2*Δ cells switched to SL medium for the specified times were measured by Western blotting. The bar-graphs represent mean±SD values for normalized relative protein amounts n=3, * $p<0.05$, *** $p<0.001$.
E) Patterns of Gln3 phosphorylation in WT and *npr2*Δ cells are distinct. Gln3 phosphorylation in WT and *npr2*Δ cells growing in YPL, YPL + 100nM Rapamycin (20 min), or over time in SL medium were measured using an SDS-PAGE gel mobility shift assay by Western blotting. The reduced mobility bands indicated higher phosphorylation.

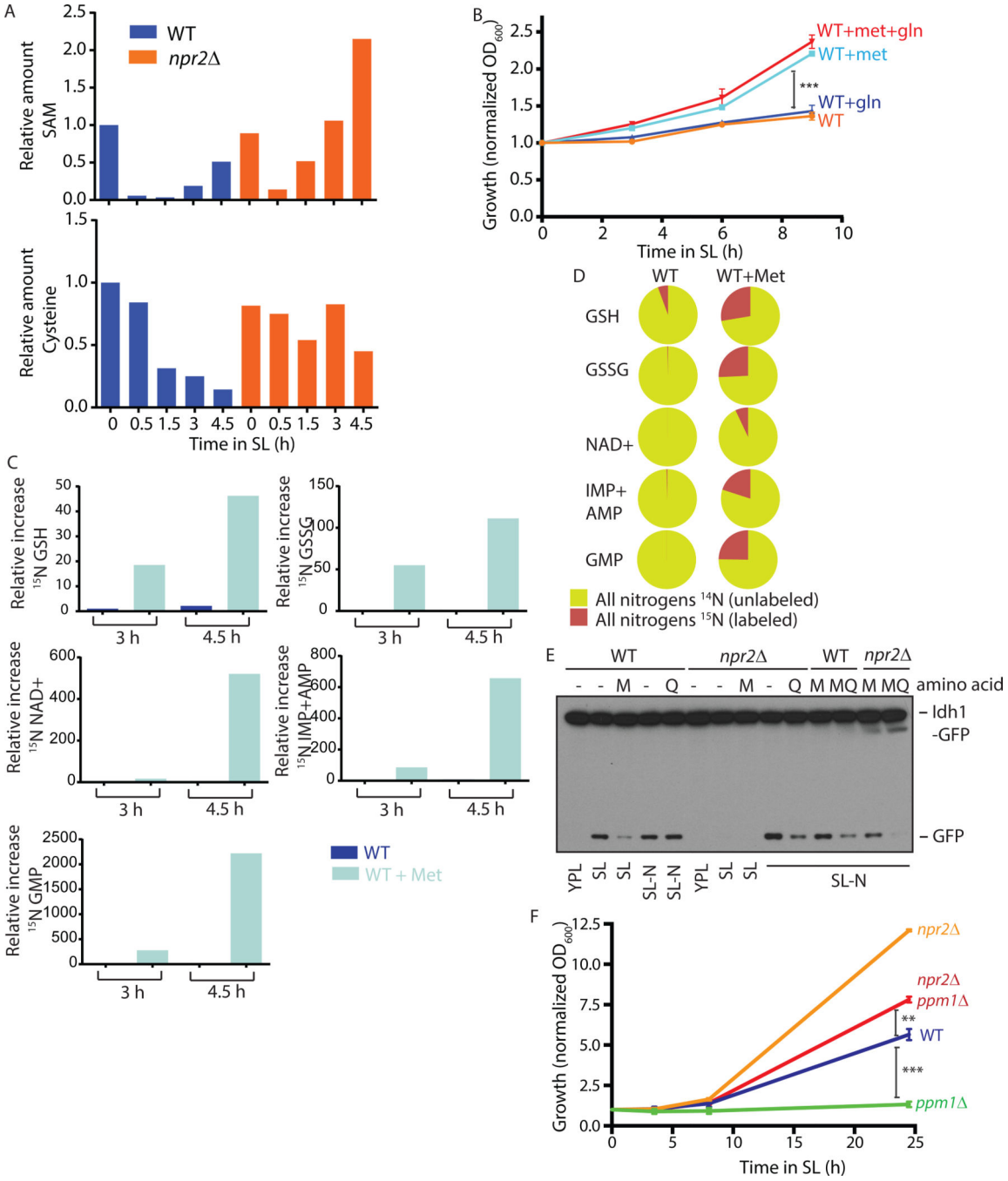

Figure 4. Methionine promotes glutamine consumption for nitrogenous metabolite biosynthesis and proliferation

A) Relative intracellular SAM and cysteine amounts in WT and *npr2*Δ cells growing in minimal (SL) medium over a 4.5 h period. Note: *npr2*Δ cells recovered rapidly from SAM and cysteine starvation, compared to WT cells.

B) Methionine promotes cell proliferation in SL medium. The panel shows growth curves for WT cells in SL medium in the presence or absence of 0.5 mM methionine, further supplemented with glutamine. n=3, mean±SD, *** $p<0.001$.

C) Ammonium incorporation into glutamine derived nitrogenous metabolites increases upon methionine supplementation. WT cells were switched from YPL to SL medium ± 0.5 mM methionine, containing ^{15}N ammonium sulfate as the nitrogen source, and relative changes in ^{15}N glutathione, NAD^+ and nucleotides were measured from cells collected at the specified times using LC-MS/MS as shown in Figure 2D (also see Supplemental Figure 3). The changes in ^{15}N metabolites are shown relative to amounts of these metabolites in WT cells 3 h after switching to SL medium.

D) Fractions of the specific nitrogenous metabolites with all nitrogens unlabeled (^{14}N), or ^{15}N labeled (newly synthesized) in WT cells in SL medium or SL medium+methionine 4.5 h after switching to SL medium with ^{15}N ammonium sulfate as the sole nitrogen source.

E) Induction of NNS (methionine starvation) and nitrogen starvation-dependent autophagy in WT and *npr2*Δ cells. WT or *npr2*Δ cells were transferred from YPL to SL medium, or SL-N medium, with or without glutamine (Q) or methionine (M) supplementation. The Western blots show the accumulation of free GFP (from the Idh1-GFP cleavage autophagy assay), which was used to detect autophagy induction.

F) Loss of the PP2A methyltransferase Ppm1 compromises growth of both WT and *npr2*Δ cells. Cell proliferation was measured in WT, *npr2*Δ, *ppm1*Δ, and *npr2*Δ/*ppm1*Δ cells. *npr2*Δ/*ppm1*Δ cells have decreased proliferation compared to *npr2*Δ cells, while *ppm1*Δ cells cannot proliferate. n=3, mean±SD. ** $p<0.01$, *** $p<0.001$.

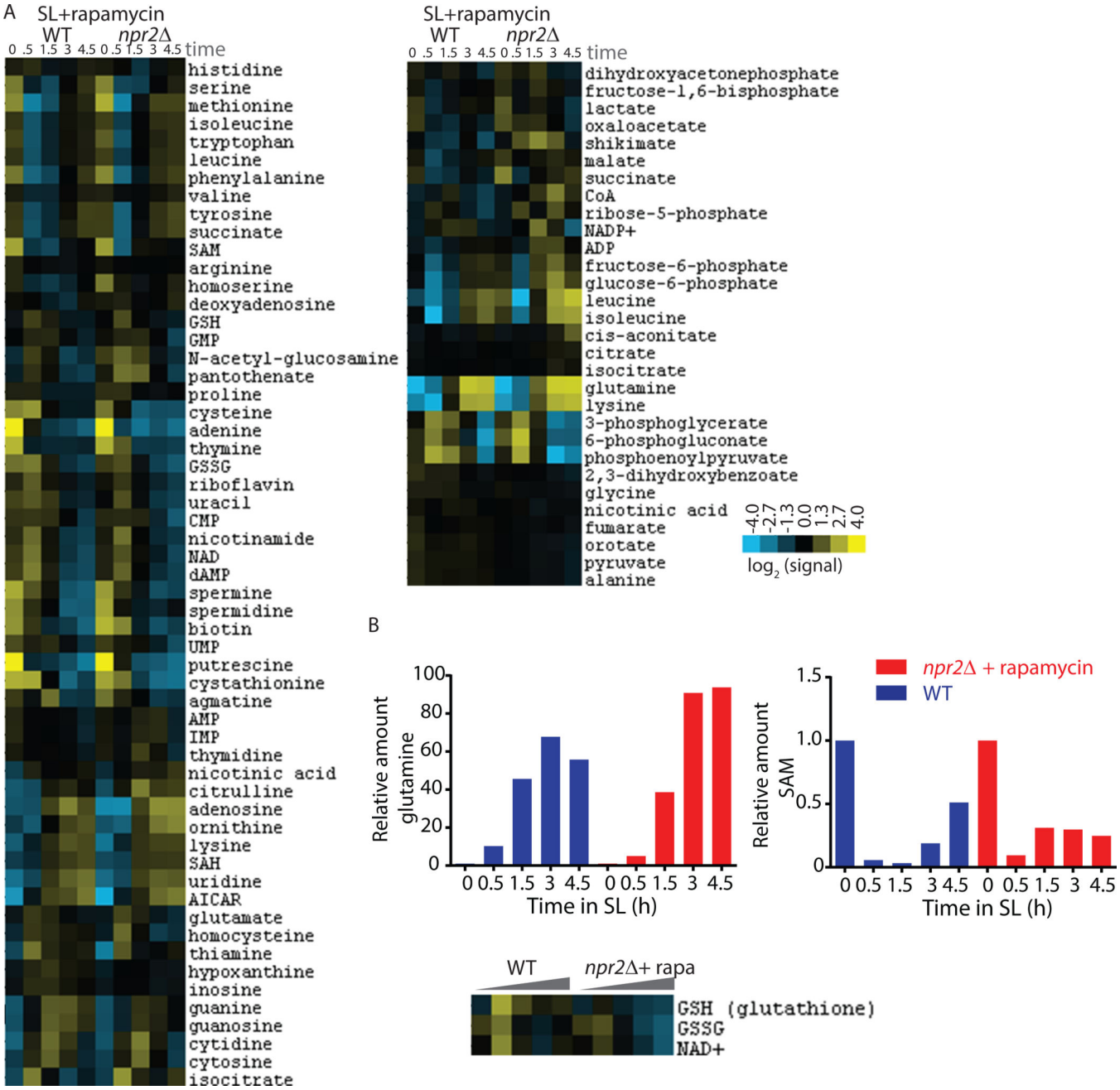

Figure 5. Changes in the metabolism of *npr2*Δ cells depend upon TORC1 activity

A) WT and *npr2*Δ growing in YPL were transferred to SL medium with 40 nM rapamycin, and intracellular metabolites measured over 4.5 h, as illustrated in the schematic on the right. Shown are hierarchical cluster analyses of changes in intracellular metabolite amounts over time in WT and *npr2*Δ cells as measured using targeted LC-MS/MS. The columns correspond to different time points (as illustrated in Figure 1C) for either WT or *npr2*Δ cells. B) Relative amounts of glutamine and SAM in WT cells growing in SL medium, and *npr2*Δ cells in SL medium + rapamycin. Note that glutamine and SAM amounts in *npr2*Δ cells in SL+rapamycin resemble WT cells in SL medium.

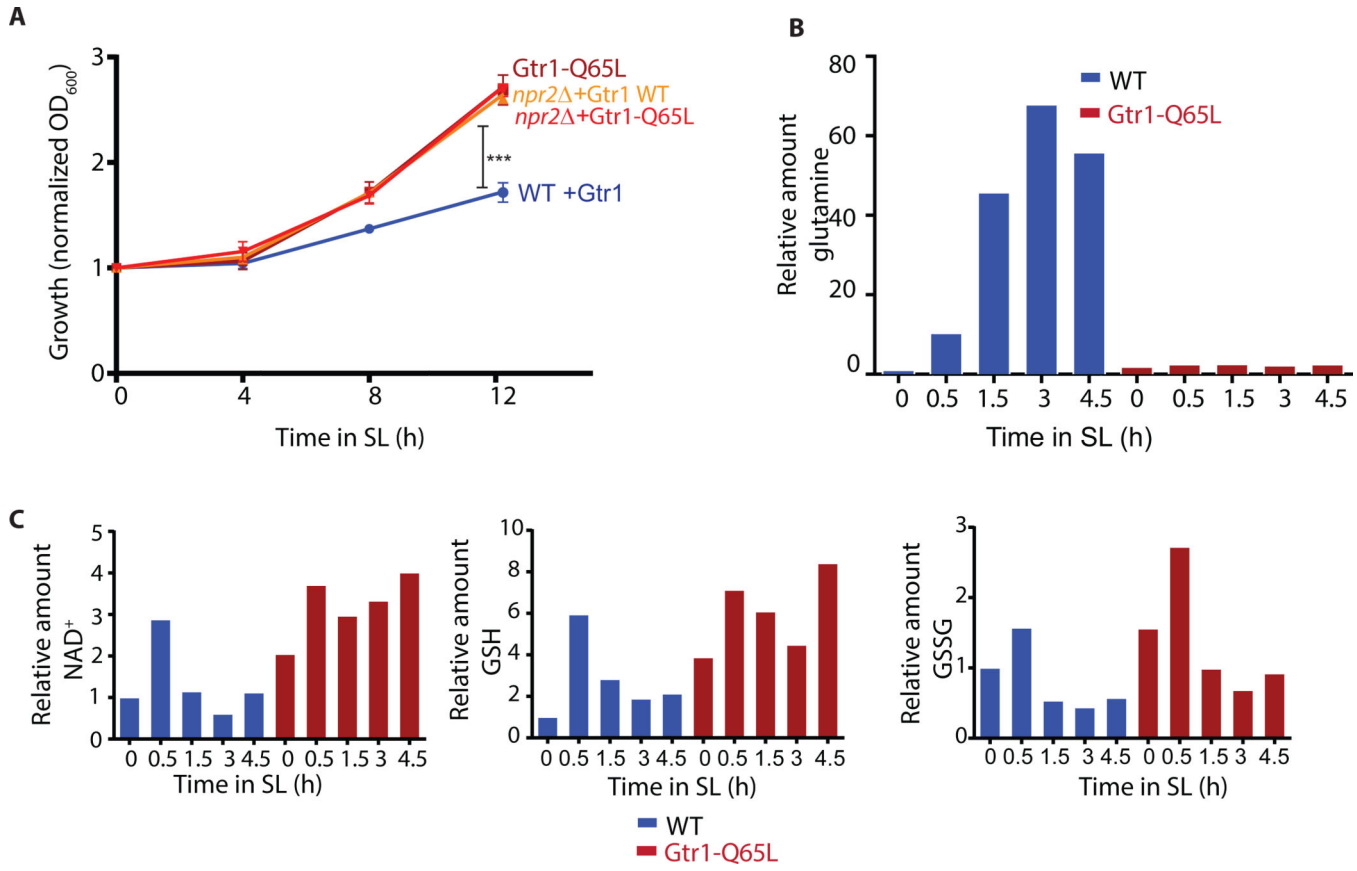

Figure 6. Increased proliferation and glutamine metabolism in *npr2*Δ cells depend upon Gtr1

A) Cells with a constitutively active form of Gtr1 (*GTR1-Q65L*) resemble *npr2*Δ cells. Shown are proliferation curves in minimal lactate (SL) medium for WT, *GTR1-Q65L* (constitutively active form of Gtr1 overexpressed), *npr2*Δ/ Gtr1-WT (WT Gtr1 expressed in the *npr2*Δ background), and *npr2*Δ/*GTR1-Q65L* cells.

B) *GTR1-Q65L* cells have low glutamine concentrations. The graphs show relative glutamine amounts in WT and GTR1-Q65L cells over a 4.5 h period growing SL medium.

C) Products of glutamine metabolism increase in *GTR1-Q65L* cells. The graphs show relative amounts of reduced glutathione (GSH), oxidized glutathione (GSSG) and NAD^+ in WT and *GTR1-Q65L* cells. Note that trends for glutamine (panel B), glutathione and NAD^+ (panel C) in *GTR1-Q65L* cells resembles that of *npr2*Δ cells (Figure 2, Table 1).

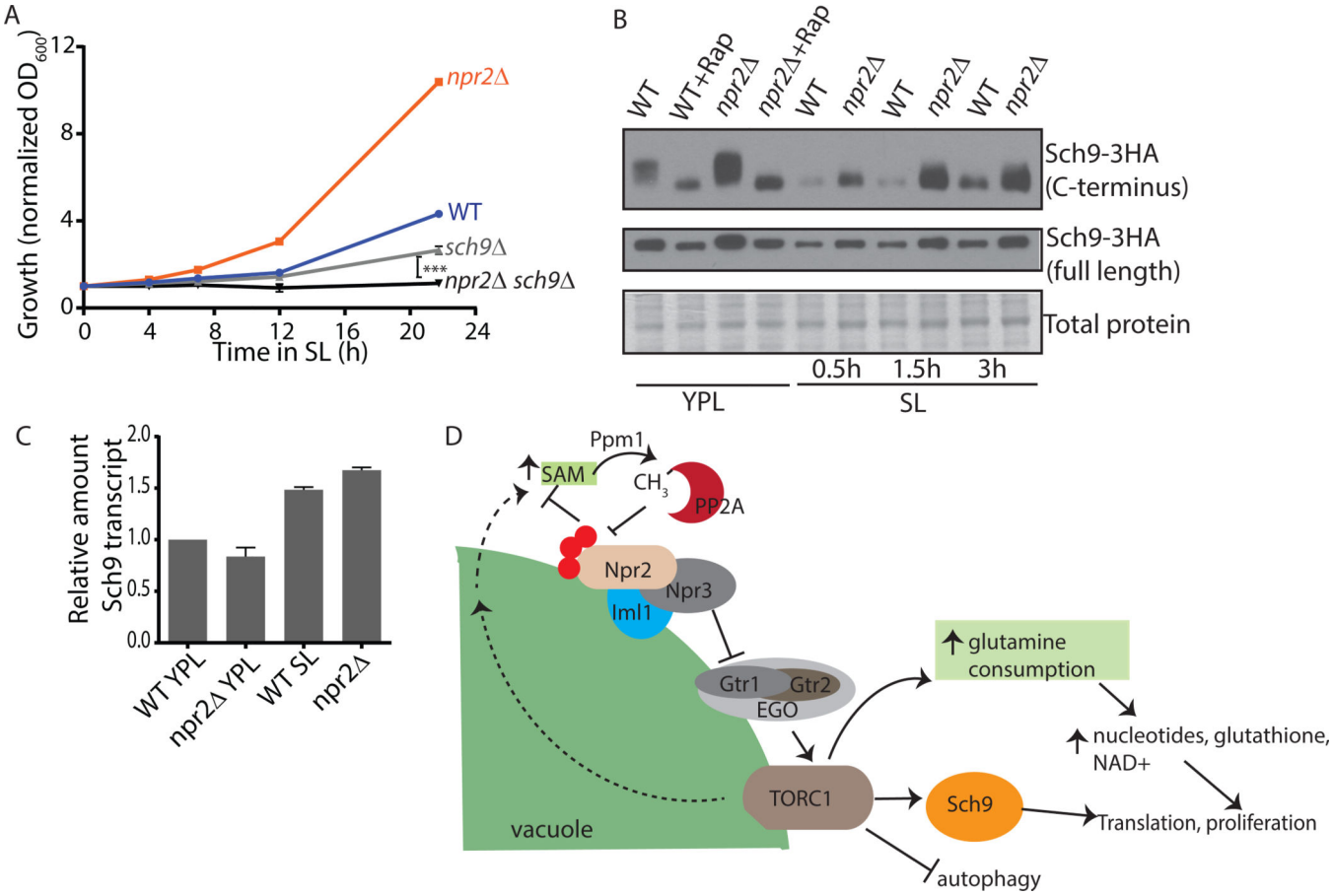

Figure 7. The S6Kinase Sch9 is required for rapid proliferation in *npr2*Δ cells

A) Proliferation curves for WT, *npr2*Δ, *sch9*Δ, and *npr2*Δ/ *sch9*Δ cells growing in minimal lactate (SL) medium are shown. Note that *npr2*Δ cells lacking Sch9 (*npr2*Δ/*sch9*Δ) grow extremely poorly in SL medium, slower than WT cells. n=3, mean±SD.

B) Sch9 phosphorylation was measured (using a chemical cleavage, Western blot based assay) in WT and *npr2*Δ cells grown in either YPL or SL medium. Note that although the Sch9 protein shows a smaller gel mobility shift in SL medium in both WT and *npr2*Δ cells compared to YPL medium, a strong increase in signal is detected in *npr2*Δ cells.

C) RT-qPCR based measurement of relative Sch9 transcript abundance in WT and *npr2*Δ cells growing in YPL or minimal SL medium. n=3, mean±SD.

D) The anti-HA antibody has a higher affinity for the C-terminally phosphorylated Sch9 protein. Upper panel: Sch9-HA tagged cells were grown in rich medium (YPD), and cells were lysed either in the presence or absence of protein phosphatase inhibitors (PPI), and processed as indicated in the schematic. Cells lysed with phosphatase inhibitors showed stronger signal in anti-HA Western blots (with uncleaved Sch9). Lower panel: Sch9 was also immunoprecipitated from cells using the HA-antibody, and treated with/without PPIs, and λ-phosphatase (λ-Ppt). Note that samples treated with λ-Phosphatase in the absence of PPI showed reduced signal intensity, compared to identical samples without λ-Phosphatase, or where PPIs were added to inhibit λ-Phosphatase.

E) A model depicting Npr2 and TORC1-mediated regulation of metabolism and cell proliferation. The absence of Npr2 results in increased TORC1 activity and proliferation through increased glutamine consumption, synergistic with increased SAM. Increased SAM can drive proliferation in part through the action of Ppm1 and methylated PP2A, which may act as a feed-forward loop further increasing TORC1 activity.

Sci Signal. Author manuscript; available in PMC 2015 June 16.

Table 1

Relative metabolite changes in WT and *npr2*Δ cells

Positive mode, Buffer A: 0.1% formic acid, Buffer B: 0.1% formic acid/100% Methanol												
Metabolite	**infusion m/z (Q1)**	**fragment m/z (Q3)**	**WT SL 0h**	**WT SL 0.5h**	**WT SL 1.5h**	**WT SL 3h**	**WT SL 4.5h**	**Δ*npr2* SL 0h**	**Δ*npr2* SL 0.5h**	**Δ*npr2* SL 1.5h**	**Δ*npr2* SL 3h**	**Δ*npr2* SL 4.5h**
methionine	150.1	104.1	1	0.068406	0.109565	0.170145	0.115072	0.8	0.075072	0.195942	0.222319	0.215362
methionine	150.1	133.0	1	0.051563	0.082031	0.137891	0.088281	0.777344	0.044922	0.162109	0.189063	0.179688
cysteine	122.0	58.9	1	0.841837	0.314796	0.25	0.145408	0.816327	0.75	0.540816	0.826531	0.45102
cysteine	122.0	76.1	1	0.664865	0.208108	0.249189	0.482162	1.254054	0.794595	0.740541	0.881081	0.767568
GSH (glutathione)	308.1	179.1	1	5.95941	2.822878	1.881919	2.140221	1.649446	6.900369	4.723247	7.896679	7.822878
GSH (glutathione)	308.1	76.1	1	5.882353	2.823529	1.872941	2.103529	1.750588	6.917647	4.4	7.6	8.047059
GSSG	613.1	231.0	1	1.565934	0.532967	0.44011	0.571429	1.192308	1.741758	0.82967	1.368132	1.406593
GSSG	613.1	177.0	1	1.624875	0.5667	0.496489	0.630893	1.334002	1.795386	0.980943	1.504514	1.464393
AMP	348.0	136.1	1	0.310423	0.233225	0.235831	0.71987	0.211075	0.286971	0.423453	0.837134	2.042345
AMP	348.0	119.2	1	0.316159	0.24356	0.228806	0.75644	0.214052	0.311475	0.470726	0.807963	2.138173
adenosine	268.1	136.0	1	0.225909	0.568182	0.590909	0.731818	0.270909	0.148182	0.234545	0.404545	1.313636
adenosine	268.1	119.1	1	0.255313	0.580381	0.6703	0.839237	0.313351	0.150409	0.267302	0.373297	1.46049
NAD+	664.0	136.2	1	2.875706	1.146893	0.60452	1.124294	0.841808	3.045198	2.514124	2.915254	4.480226
NAD+	664.0	428.0	1	2.792363	1.175418	0.571599	1.097852	0.861575	3.090692	2.613365	2.995227	4.582339
thiamine	265.0	122.1	1	8.441558	5.242031	5.714286	9.87013	0.506494	10.66116	10.89728	20.54309	17.47344
thiamine	265.0	144.1	1	7.003891	4.396887	4.785992	7.782101	0.719844	9.338521	8.44358	17.58755	13.6965
riboflavin	377.1	243.1	1	1.435	0.695	0.4365	0.7	0.6	1.17	0.585	0.835	2.665
riboflavin	377.1	172.1	1	1.537559	0.735915	0.463615	0.761737	0.778169	1.197183	0.625587	0.867371	3.086854
guanine	152.1	135.1	1	2.214592	5.150215	5.450644	6.437768	0.725322	0.600858	1.733906	0.157511	0.309442
guanine	152.1	110.2	1	2.365385	5.269231	5.903846	6.875	0.705769	0.675962	1.875	0.163462	0.358654
spermine	203.2	129.1	1	0.46978	0.414835	0.332418	0.417582	0.516484	0.46978	0.417582	0.615385	0.906593
spermine	203.2	112.1	1	0.24	0.361765	0.213235	0.326471	0.423529	0.194412	0.145588	0.444118	0.641176
nicotinic acid	124.0	80.0	1	1	1.18239	1.27673	1.742138	1.54717	2.150943	2.987421	2.308176	1.591195
nicotinic acid	124.0	77.9	1	0.651584	0.755656	1.158371	1.411765	1.171946	1.561086	1.900452	1.443439	1.027149
nicotinamide	123.0	80.0	1	1.988	0.712	0.408	0.644	1.016	2.412	1.768	2.6	3.912
nicotinamide	123.0	78.1	1	2.281947	0.728195	0.471602	0.560852	0.864097	2.647059	1.906694	3.144016	3.711968
arginine	175.1	70.1	1	0.762542	0.658863	0.692308	0.946488	0.725753	0.829431	1.294314	1.301003	1.006689

Positive mode, Buffer A: 0.1% formic acid, Buffer B: 0.1% formic acid/100% Methanol

Metabolite	infusion m/z (Q1)	fragment m/z (Q3)	WT SL 0h	WT SL 0.5h	WT SL 1.5h	WT SL 3h	WT SL 4.5h	Δ*npr2* SL 0h	Δ*npr2* SL 0.5h	Δ*npr2* SL 1.5h	Δ*npr2* SL 3h	Δ*npr2* SL 4.5h
histidine	156.1	110.0	1	1.455521	0.707055	0.881902	1.242331	1.355828	1.009202	0.496933	0.77454	0.430982
histidine	156.1	83.2	1	1.391304	0.7	0.847826	1.23913	1.297101	0.956522	0.461594	0.753623	0.414493
lysine	147.1	84.1	1	2.911765	5.598039	6.411765	4.892157	0.978431	1.647059	2.186275	3.186275	1.980392
lysine	147.1	130.1	1	3.871473	8.009404	9.200627	6.630094	1.007837	1.865204	2.554859	3.213166	1.974922
phenylalanine	166.1	120.1	1	0.103552	0.159311	0.262648	0.271259	0.904198	0.102045	0.175457	0.125942	0.11733
phenylalanine	166.1	103.2	1	0.106377	0.153913	0.248986	0.269855	0.913043	0.098261	0.171304	0.122899	0.116522
proline	116.0	70.1	1	1.078261	1.526087	1.943478	1.7	3.630435	5.217391	3.678261	2.413043	1.56087
proline	116.0	69.0	1	1.039604	1.554455	1.930693	1.742574	3.693069	5.346535	3.782178	2.39604	1.519802
serine	106.0	60.1	1	0.235088	0.228947	0.30614	0.242105	1.122807	0.458772	0.638596	0.703509	0.759649
serine	106.0	88.0	1	2.818182	1.441558	1.011688	1.136364	1.506494	3.051948	3.051948	2.961039	3.480519
tyrosine	182.1	136.1	1	0.196154	0.237821	0.4	0.396154	0.903846	0.170513	0.257051	0.178846	0.189103
tyrosine	182.1	91.0	1	0.189344	0.227049	0.389344	0.37459	0.885246	0.161475	0.245082	0.159836	0.161475
glutamate	148.1	84.1	1	3.957055	2.815951	2.40184	2.076687	1.518405	2.711656	2.42638	2.015337	1.754601
glutamate	148.1	130.1	1	3.871622	2.804054	2.405405	2	1.52027	2.682432	2.337838	1.986486	1.554054
tryptophan	205.1	188.2	1	0.171141	0.263087	0.393289	0.501342	0.872483	0.201342	0.328188	0.267785	0.25302
tryptophan	205.1	146.2	1	0.164356	0.251485	0.382178	0.452475	0.811881	0.141584	0.254455	0.189109	0.178218
valine	118.1	72.1	1	0.481982	0.594595	0.684685	0.563063	0.932432	0.366216	0.468468	0.381982	0.354054
valine	118.1	55.0	1	0.464286	0.59472	0.661491	0.531056	0.92236	0.361801	0.481366	0.385093	0.32764
adenine	136.0	119.0	1	0.021165	0.002291	0.001746	0.203883	0.761165	0.021553	0.011515	0.029515	0.061553
adenine	136.0	92.2	1	0.025344	0.005565	0.003595	0.182443	0.656489	0.019084	0.020916	0.01855	0.071908
ornithine	133.1	70.1	1	0.404566	1.305936	2.479452	3.187215	0.570776	0.538813	1.767123	1.821918	1.324201
ornithine	133.1	116.0	1	0.468421	1.578947	3.045113	3.977444	0.781955	0.545865	1.947368	2.112782	1.556391
cytidine	244.1	112.2	1	2.67094	4.594017	2.307692	0.65812	0.700855	0.715812	2.991453	0.122222	0.166453
cytidine	244.1	95.2	1	2.415197	5.535957	2.184532	0.767978	0.822252	0.660787	3.012212	0.071913	0.234735
GMP	364.0	152.0	1	0.376068	0.210541	0.150997	0.470085	0.144444	0.347578	0.404558	0.609687	1.723647
GMP	364.0	135.2	1	0.383594	0.223438	0.147656	0.430469	0.142969	0.355469	0.414063	0.626563	1.890625
homoserine	120.0	74.0	1	0.438608	0.336076	0.277215	0.151899	1.949367	0.968354	0.816456	0.829114	0.501899
homoserine	120.0	56.2	1	0.440196	0.327451	0.252941	0.136275	2.009804	0.916667	0.756863	0.731373	0.476471
cystathionine	223.1	88.0	1	1.147097	0.176774	0.091871	0.091742	1.445161	1.110968	0.205161	0.247742	0.291613
cystathionine	223.1	134.1	1	1.092398	0.222222	0.100936	0.111813	1.567251	1.181287	0.224561	0.277193	0.288889

Metabolite	infusion m/z (Q1)	fragment m/z (Q3)	WT SL 0h	WT SL 0.5h	WT SL 1.5h	WT SL 3h	WT SL 4.5h	Δ*npr2* SL 0h	Δ*npr2* SL 0.5h	Δ*npr2* SL 1.5h	Δ*npr2* SL 3h	Δ*npr2* SL 4.5h
Positive mode, Buffer A: 0.1% formic acid, Buffer B: 0.1% formic acid/100% Methanol												
SAM	399.1	250.2	1	0.057119	0.033729	0.188983	0.511864	0.889831	0.139831	0.516949	1.059322	2.152542
SAM	399.1	136.0	1	0.047153	0.034698	0.14395	0.535587	0.925267	0.131495	0.551601	0.905694	2.224199
spermidine	146.2	72.1	1	0.965174	1.004975	0.651741	2.084577	1.422886	1.268657	1.263682	0.59204	0.81592
spermidine	146.2	84.0	1	0.963636	0.835455	0.537273	1.554545	1	1.1	1.072727	0.446364	0.596364
succinate	119.0	91.0	1	0.208429	0.246743	0.40613	0.378927	0.850575	0.162069	0.239847	0.180077	0.167816
succinate	119.0	65.0	1	0.163636	0.183333	0.279545	0.293939	0.901515	0.163636	0.208333	0.110606	0.133333
IMP	349.0	137.1	1	0.851301	0.780669	0.553903	0.129368	1.01487	0.401487	1.460967	3.977695	3.137546
IMP	349.0	97.1	1	0.56546	0.941504	0.668524	0.952646	0.947075	0.231755	1.231198	3.844011	2.952646
SAH	385.1	136.2	1	1.021368	1.99359	2.393162	2.15812	0.730769	0.643162	1.74359	1.147436	1.803419
SAH	385.1	134.0	1	1.03163	2.311436	2.822384	2.603406	0.720195	0.737226	2.092457	1.316302	2.097324
citrulline	176.0	159.2	1	2.721239	7.367257	4.004425	3.163717	1.132743	7.5	10.95133	14.22566	6.460177
citrulline	176.0	70.1	1	1.4	2.55	1.716667	1.75	1.033333	2.875	4.05	5.3	2.583333
hypoxanthine	137.0	110.0	1	1.902597	1.905844	1.720779	1.496753	1.746753	1.506494	0.980519	0.151623	0.077597
hypoxanthine	137.0	119.2	1	1.885417	1.916667	1.767361	1.545139	1.760417	1.548611	1.055556	0.182639	0.086806
cytosine	112.0	95.0	1	2.766667	3.966667	1.525	0.734167	0.941667	0.521667	2.291667	0.246667	0.215
guanosine	284.0	152.1	1	2.44143	5.696671	6.128237	7.053021	0.768187	0.659679	1.849568	0.048829	0.091122
guanosine	284.0	135.1	1	2.415541	5.574324	6.216216	7.162162	0.790541	0.679054	1.922297	0.062162	0.084122
inosine	268.9	137.2	1	3.314961	4.409449	4.685039	5.811024	1.409449	1.929134	2.771654	0.040866	0.044488
inosine	268.9	110.0	1	3.186667	4.446667	4.54	5.8	1.386667	1.853333	2.786667	0.0346	0.0394
uridine	245.0	112.9	1	2.156028	7.304965	11.20567	7.801418	1	0.542553	5.205674	0.258156	0.131915
dAMP	332.1	81.0	1	1.915638	1.718107	1.176955	1.32716	1.100823	2.757202	2.489712	2.345679	2.572016
CMP	324.1	112.2	1	1.043379	1.237443	1.589041	1.504566	0.563927	1.184932	0.815068	1.776256	3.127854
putrescine	89.1	72.0	1	0.020492	0.021967	0.022377	0.025902	0.784426	0.034098	0.032459	0.023525	0.018115
putrescine	89.1	71.0	1	0.639098	0.81203	0.575188	0.447368	0.800752	1.011278	1.015038	0.766917	0.672932
dGMP	348.1	152.2	1	3.638554	2.089157	3.228916	3.759036	1.207229	4.216867	2.375904	4.819277	6.024096
dCMP	308.1	112.0	1	0.820856	0.572193	0.590909	0.668449	0.780749	0.933155	0.516043	1.540107	1.141711
Positive mode, Buffer A: 5mM Ammonium Acetate pH 5.0, Buffer B: 5mM Ammonium Acetate/100% methanol												
FMN	456.9	243.2	1	2.344434	1.467694	2.818701	3.987379	2.42918	1.654821	4.299164	4.122706	2.026148
FMN	456.9	172.3	1	3.051871	1.932879	3.324017	5.335181	3.285905	2.116272	5.684883	6.492486	3.014261
FAD	785.9	348.1	1	1.888318	1.120633	2.289957	3.151763	2.246339	1.197312	3.5928	3.877098	1.116822

Positive mode, Buffer A: 0.1% formic acid, Buffer B: 0.1% formic acid/100% Methanol

Metabolite	infusion m/z (Q1)	fragment m/z (Q3)	WT SL 0h	WT SL 0.5h	WT SL 1.5h	WT SL 3h	WT SL 4.5h	Δ*npr2* SL 0h	Δ*npr2* SL 0.5h	Δ*npr2* SL 1.5h	Δ*npr2* SL 3h	Δ*npr2* SL 4.5h
FAD	785.9	136.0	1	1.955	1.191829	2.275213	3.148234	2.188366	1.203342	3.527817	3.952292	1.311196
acetyl-CoA	809.9	303.2	1	1.607554	1.99143	2.811967	3.196067	1.317156	1.776968	2.185983	1.585406	2.807223
acetyl-CoA	809.9	159.2	1	1.796172	1.953379	2.981258	2.971771	1.470304	1.798278	2.393571	1.546524	2.898084
NADP+	743.9	136.0	1	1.649148	1.363462	1.396452	1.053677	2.45663	1.581637	3.268954	3.262334	0.290374
NADP+	743.9	232.1	1	1.571544	1.575264	1.223941	1.148167	2.766447	1.605187	2.58209	3.01053	0.273274
ADP	428.0	136.0	1	1.40721	0.728005	0.511313	0.457187	1.53816	0.816226	0.91077	1.063037	0.714079
ADP	428.0	119.0	1	1.369416	0.641659	0.576471	0.449447	1.513667	0.751514	0.978397	1.220639	0.565973
TPP	425.0	122.0	1	3.276937	2.135025	3.489177	4.449426	2.131526	1.842945	3.030984	3.276506	0.446729
TPP	425.0	304.2	1	3.418977	2.06813	3.729345	4.710261	2.27373	1.925802	3.585796	3.547882	0.422581
aspartate	134.1	74.1	1	0.852238	0.868615	0.702388	0.579255	0.248043	0.550993	0.221738	0.333578	0.433984
aspartate	134.1	88.0	1	0.908737	0.746695	0.65682	0.532172	0.259559	0.498016	0.209491	0.302058	0.417307
UDP	404.9	96.9	1	0.962967	0.602891	0.596671	0.622153	0.997385	0.809712	0.646142	0.678688	0.258658
UDP	404.9	69.1	1	1.071249	0.622504	0.572431	0.743527	1.086555	0.852754	0.764726	0.628575	0.280436
UDP-glucose	584.0	405.1	1	0.736783	0.579879	0.422957	0.480838	0.945512	1.082349	0.596431	0.523786	0.243156
UDP-glucose	584.0	97.0	1	0.707278	0.479944	0.359985	0.405878	0.998687	0.976699	0.507954	0.506737	0.205273
UDP-N-acetylglucosamine	608.0	204.1	1	0.6432	0.488118	0.235934	0.226213	0.699997	0.538255	0.309244	0.326776	0.387451
UDP-N-acetylglucosamine	608.0	138.0	1	0.688363	0.617835	0.293916	0.249105	0.800207	0.672961	0.394946	0.375213	0.41088
glucosamine	180.2	162.2	1	0.613874	0.526334	0.504592	0.436438	0.723323	0.683328	0.723303	0.747406	0.157182
glucosamine	180.2	72.2	1	0.691845	0.614707	0.547647	0.484596	0.738672	0.704129	0.842072	0.779036	0.146913
threonine	120.1	74.0	1	0.354667	0.1707	0.193791	0.155491	0.409714	0.25546	0.172026	0.20031	0.503184
threonine	120.1	56.0	1	0.295463	0.187929	0.209583	0.123901	0.397614	0.234068	0.126795	0.185493	0.610049
CoA	768.0	261.2	1	0.88862	0.864523	0.788852	1.269752	0.452583	0.873878	0.691223	0.587389	2.669135
ATP	508.0	136.2	1	1.432887	0.790715	0.197233	0.266496	2.2705	1.217267	0.467305	0.353149	0.465343
ATP	508.0	410.1	1	1.342654	0.772228	0.249069	0.201802	1.985089	1.135825	0.517593	0.369807	0.461073
CTP	484.2	112.2	1	3.266674	2.31318	2.113714	1.918097	3.547908	2.788644	2.685718	0.924285	0.651103
UTP	485.0	97.1	1	1.624351	1.126434	0.729648	0.694419	1.657803	1.14639	0.788406	0.39878	1.269605
UTP	485.0	69.1	1	2.117972	1.314542	0.800891	1.150024	2.064177	1.67047	1.008374	0.674641	1.830568
CDP	404.0	112.0	1	1.68484	1.100577	1.559817	1.966208	1.587432	1.110605	1.400682	1.169237	0.383994
GTP	523.8	152.1	1	1.688384	1.070047	0.694985	0.757289	2.944169	1.471438	1.856898	0.960524	0.846243
GTP	523.8	135.0	1	1.920529	1.376923	0.848756	0.898426	3.130265	1.882959	2.148878	1.16801	0.865345

Metabolite	infusion m/z (Q1)	fragment m/z (Q3)	WT SL 0h	WT SL 0.5h	WT SL 1.5h	WT SL 3h	WT SL 4.5h	Δ*npr2* SL 0h	Δ*npr2* SL 0.5h	Δ*npr2* SL 1.5h	Δ*npr2* SL 3h	Δ*npr2* SL 4.5h
Positive mode, Buffer A: 0.1% formic acid, Buffer B: 0.1% formic acid/100% Methanol												
GDP	443.9	152.1	1	1.543517	0.962583	1.044175	1.374779	1.908206	1.106285	2.136696	2.938664	0.439638
GDP	443.9	135.0	1	1.527349	0.856177	0.965476	1.183242	1.860746	0.895874	2.026838	2.856226	0.269443
Negative mode, Buffer A: 5mM Tributyl amine, Buffer B: 100% methanol												
3-phosphoglycerate	185.0	78.9	1	6.561265	5.928854	4.822134	4.486166	0.365613	5.948617	4.762846	4.249012	4.011858
3-phosphoglycerate	185.0	96.9	1	6.533613	5.92437	4.726891	4.348739	0.529412	5.92437	4.87395	4.348739	4.138655
ADP	426.0	78.8	1	0.673835	0.684588	0.602151	1.709677	0.978495	0.845878	0.784946	1.035842	1.835125
ADP	426.0	158.9	1	0.719512	0.552846	0.565041	1.630081	0.593496	0.739837	0.686992	0.96748	2.004065
a-ketoglutarate	144.9	100.9	1	1.13	1.84	3.5	4.77	1.22	3.05	3.38	3.38	1.722107
a-ketoglutarate	144.9	56.8	1	2.41	4.11	8.28	12.1	2.38	8.06	8.91	8.91	2.999056
cis-aconitate	172.9	85.0	1	2.18328	2.5209	2.59164	2.845659	0.935691	1.585209	2.289389	1.350482	1.697749
cis-aconitate	172.9	129.0	1	2.152027	2.304054	2.516892	2.736486	0.983108	1.466216	2.168919	1.341216	1.665541
citrate	191.0	110.9	1	2.69837	2.907609	2.491848	3.233696	1.396739	2.17663	2.649457	2.024457	2.442935
citrate	191.0	87.0	1	3.15544	2.92228	2.544041	3.321244	1.414508	2.181347	2.601036	1.860104	2.544041
CoA	766.2	79.1	1	11.80782	13.92508	16.44951	34.52769	10.30945	18.56678	14.67427	23.12704	50
CoA	766.2	408.0	1	30.14925	24.47761	31.71642	68.8806	16.86567	26.41791	27.08955	37.61194	82.08955
DHAP	168.9	96.9	1	1.426136	1.488636	0.903409	2.022727	0.475568	2.221591	1.744318	1.772727	3.636364
DHAP	168.9	78.9	1	1.581818	1.654545	0.882727	2.354545	0.439091	2.5	1.818182	1.754545	3.845455
fructose-1,6-bisphosphate	338.9	78.8	1	1.717842	1.128631	0.863071	3.585062	0.634855	2.701245	1.323651	2.493776	4.232365
fructose-1,6-bisphosphate	338.9	96.8	1	1.6	0.941176	0.641176	4.776471	0.466471	2.917647	1.452941	2.517647	5.858824
fructose-6-phosphate	258.9	78.9	1	1.550157	2.460815	4.294671	11.0815	1.159875	4.216301	4.60815	5.987461	4.059561
fructose-6-phosphate	258.9	169.0	1	1.554745	3.361314	5.875912	13.54015	1.521898	5.328467	5.656934	8.686131	4.270073
fumarate	114.9	71.1	1	0.867826	1.017391	1.017391	0.806087	1.330435	1.226087	1.417391	0.947826	0.622609
fumarate	114.9	70.0	1	0.599286	0.757143	0.721429	0.642857	0.9	0.914286	1.164286	0.685714	0.422857
glucose-6-phosphate	258.9	97.0	1	1.823322	3.289753	5.583039	20	1.381625	6.855124	7.526502	7.844523	4.381625
glucose-6-phosphate	258.9	199.0	1	0.991803	1.981557	3.811475	10.77869	0.946721	3.852459	4.32377	5.696721	2.868852
isocitrate	191.0	111.0	1	2.418033	2.540984	2.336066	2.315574	1.532787	2.069672	2.397541	2.131148	2.479508
isocitrate	191.0	73.0	1	2.872483	2.231544	2.540268	4.026846	1.533557	6.073826	8.389262	3.825503	2.389262
lactate	88.9	43.0	1	0.344138	0.27931	0.218966	0.431034	0.486207	0.32069	0.266207	0.23	0.47931
lactate	88.9	71.1	1	0.34	0.289048	0.220476	0.440476	0.5	0.339048	0.279524	0.24	0.504762

Positive mode, Buffer A: 0.1% formic acid, Buffer B: 0.1% formic acid/100% Methanol

Metabolite	infusion m/z (Q1)	fragment m/z (Q3)	WT SL 0h	WT SL 0.5h	WT SL 1.5h	WT SL 3h	WT SL 4.5h	Δ*npr2* SL 0h	Δ*npr2* SL 0.5h	Δ*npr2* SL 1.5h	Δ*npr2* SL 3h	Δ*npr2* SL 4.5h
malate	132.9	114.9	1	0.596078	1.360784	1.047059	0.929412	1.058824	1.737255	2.223529	1.101961	0.427451
malate	132.9	71.0	1	0.598058	1.407767	1.067961	0.950485	1.07767	1.757282	2.252427	1.07767	0.416505
NADP+	742.1	620.2	1	2.844444	2.604444	1.4	4.488889	1.12	3.853333	2.582222	2.68	6.133333
NADP+	742.1	78.9	1	2.629559	1.752399	1.086372	3.493282	1.06334	3.090211	2.380038	2.226488	5.777351
orotate	154.9	110.9	1	0.540426	0.519149	0.519149	0.4	0.787234	0.553191	0.502128	0.551064	0.52766
oxaloacetate	130.9	87.0	1	0.588402	1.015559	0.574257	2.234795	0.635078	2.192362	1.824611	0.889675	0.792079
nicotinic acid	121.9	78.0	1	0.390127	0.283439	0.326433	0.296178	0.753185	0.393312	0.515924	0.402866	0.386943
phosphoenoylpyruvate	166.9	78.9	1	18.45161	18.12903	13.74194	9.612903	1.058065	14.51613	12.32258	9.419355	3.63871
6-phosphogluconate	274.9	78.9	1	8.833333	4.25	2.7625	5.333333	0.775	13.125	3.7625	5.541667	6.083333
6-phosphogluconate	274.9	97.0	1	8.5	3.5	2.0375	4.78125	0.884375	13.3125	3.046875	5.5	6.3125
ribose-5-phosphate	228.9	79.1	1	1.720991	1.994785	2.894394	3.233377	1.172099	1.642764	1.642764	1.603651	1.747066
ribose-5-phosphate	228.9	96.9	1	2.459827	1.928307	2.10136	2.645241	0.887515	1.31026	1.421508	1.359703	1.594561
shikimate	172.9	93.0	1	2.26393	2.419355	2.234604	2.917889	1.469208	2.252199	2.478006	1.929619	2.14956
alanine	88.0	88.0	1	0.546875	0.484896	0.5625	0.385938	0.786458	0.572917	0.53125	0.480208	0.546875
glycine	74.0	74.0	1	0.417647	0.500535	0.413369	0.45508	0.68984	0.433155	0.32139	0.493048	0.458289
succinate	116.9	73.0	1	0.122992	0.372576	0.297784	0.360111	3.739612	0.411357	1.17867	0.698061	0.249307
succinate	116.9	99.0	1	0.135938	0.460156	0.384375	0.382813	4.265625	0.460156	1.335938	0.890625	0.321094
pyruvate	86.9	86.9	1	0.591736	0.565289	0.403306	0.299174	0.814876	0.484298	0.479339	0.317355	0.295868
pyruvate	86.9	43.0	1	0.494737	0.763158	0.739474	1.15	0.815789	0.855263	0.839474	0.65	0.826316
leucine	130.0	84.0	1	0.339048	0.638095	0.561905	0.561905	0.871429	0.542857	0.314286	0.185714	0.045524
isoleucine	130.0	82.1	1	0.391364	0.55	0.781818	0.399545	0.663636	0.266818	0.275909	0.225455	0.199091
isoleucine	130.0	45.2	1	0.149677	0.190323	0.230968	0.243871	0.418065	0.043935	0.064129	0.118065	0
glutamine	144.9	127.2	1	10.32419	45.63591	67.83042	55.86035	1.533666	3.291771	3.142145	1.832918	1.533666
glutamine	144.9	109.0	1	19.71429	88.57143	131.9048	106.1905	2.5	6.619048	5.952381	3.061905	2.566667
lysine	144.9	97.0	1	1.009615	3.557692	5.692308	5.413462	0.953846	0.702885	0.831731	0.878846	0.472115
UDP	402.0	110.0	1	1.691652	1.352641	1.46678	1.720613	0.829642	1.218058	0.923339	0.739353	0.701874
UDP	402.0	158.0	1	1.805556	1.305556	1.537037	1.833333	0.848148	1.166667	0.944444	0.746296	0.737963

Sci Signal. Author manuscript; available in PMC 2015 June 16.

Table 2

Relative metabolite changes in WT and *npr2*Δ cells growing in SL medium + 40 nM rapamycin

Positive mode, Buffer A: 0.1% formic acid, Buffer B: 0.1% formic acid/100% Methanol												
Metabolite	**infusion m/z (Q1)**	**fragment m/z (Q3)**	**WT SL+0h**	**WT SL+R 0.5h**	**WT SL+R 1.5h**	**WT SL+R 3h**	**WT SL+R 4.5h**	**Δ*npr2* SL 0h**	**Δ*npr2* SL 0.5h**	**Δ*npr2* SL 1.5h**	**Δ*npr2* SL 3h**	**Δ*npr2* SL 4.5h**
methionine	150.1	104.1	1	0.075358	0.133238	0.366762	0.441261	1.34384	0.070487	0.269054	0.561605	0.561605
methionine	150.1	133.0	1	0.080866	0.146931	0.350542	0.404332	1.270758	0.080505	0.270758	0.555957	0.534296
cysteine	122.0	58.9	1	1.140187	0.35514	0.249221	0.252025	0.875389	0.370717	0.117757	0.139875	0.137383
cysteine	122.0	76.1	1	0.584314	0.419608	0.266667	0.286275	1.172549	0.654902	0.198824	0.199608	0.266275
GSH (glutathione)	308.1	179.1	1	2.029126	1.519417	0.936893	0.927184	1.18932	2.247573	1.247573	0.966019	0.873786
GSH (glutathione)	308.1	76.1	1	2.041667	1.446429	0.904762	0.952381	1.089286	2.172619	1.178571	0.982143	0.89881
GSSG	613.1	231.0	1	1.07804	0.497278	0.239564	0.190563	0.644283	0.756806	0.335753	0.192377	0.147005
GSSG	613.1	177.0	1	1.169329	0.501597	0.227796	0.199361	0.859425	1.038339	0.332268	0.224281	0.140575
AMP	348.0	136.1	1	0.727642	0.721951	0.66748	0.512195	0.869919	0.682927	0.95935	1.04065	0.50813
AMP	348.0	119.2	1	0.780347	0.745665	0.687861	0.534104	0.942197	0.699422	1.040462	1.052023	0.513873
adenosine	268.1	136.0	1	1.057082	4.365751	7.44186	4.693446	0.542283	0.530655	4.365751	8.171247	8.044397
adenosine	268.1	119.1	1	1.0625	5.03125	7.875	5.2	0.568125	0.51125	4.68125	9	8.75
NAD+	664.0	136.2	1	1.622222	0.723704	0.362222	0.275556	0.814815	1.214815	0.681481	0.468889	0.286667
NAD+	664.0	428.0	1	1.355	0.823333	0.316667	0.295	0.88	1.553333	0.72	0.443333	0.288333
thiamine	265.0	122.1	1	5.573427	3	2.552448	2.72028	0.526573	4.440559	1.853147	2.041958	2.594406
thiamine	265.0	144.1	1	5.045662	2.60274	2.018265	2.351598	0.440639	3.424658	1.586758	1.60274	2.06621
riboflavin	377.1	243.1	1	1.560241	0.855422	0.63253	0.521687	0.837349	1.156627	0.680723	0.501205	0.385542
riboflavin	377.1	172.1	1	1.692913	0.934383	0.643045	0.574803	0.843832	1.085302	0.64042	0.489501	0.412073
guanine	152.1	135.1	1	2.22619	5.410714	5.297619	3.904762	1.059524	1.755952	3.904762	3.52381	2.452381
guanine	152.1	110.2	1	2.116705	5.034325	4.713959	3.832952	0.911899	1.773455	3.695652	3.26087	2.517162
spermine	203.2	129.1	1	0.490196	0.278867	0.096514	0.085621	0.869281	0.372549	0.198911	0.101307	0.116558
spermine	203.2	112.1	1	0.337526	0.145702	0.050943	0.034591	0.733753	0.155765	0.080503	0.056813	0.093711
UMP	325.0	97.0	1	0.690867	0.770492	0.477752	0.305621	0.891101	0.655738	0.593677	0.387588	0.225995
UMP	325.0	212.9	1	0.671001	0.745124	0.478544	0.338101	0.890767	0.694408	0.624187	0.418726	0.215865
N-acetyl-glucosamine	222.1	138.1	1	2.7125	1.88125	0.775	1.03125	2.6875	3.74375	2.78125	1.33125	0.98125
nicotinic acid	124.0	80.0	1	2.596491	1.929825	2.114035	2.359649	1.263158	1.885965	2.552632	2.473684	3.157895
nicotinic acid	124.0	77.9	1	1.859155	1.739437	1.422535	1.788732	1.084507	2.704225	1.711268	1.816901	2.176056

Positive mode, Buffer A: 0.1% formic acid, Buffer B: 0.1% formic acid/100% Methanol

Metabolite	infusion m/z (Q1)	fragment m/z (Q3)	WT SL+0h	WT SL+R 0.5h	WT SL+R 1.5h	WT SL+R 3h	WT SL+R 4.5h	Δ*npr2* SL 0h	Δ*npr2* SL 0.5h	Δ*npr2* SL 1.5h	Δ*npr2* SL 3h	Δ*npr2* SL 4.5h
nicotinamide	123.0	80.0	1	1.663934	0.79918	0.396311	0.340574	0.852459	1.762295	0.721311	0.446721	0.380738
nicotinamide	123.0	78.1	1	2.067757	1.005841	0.494159	0.456776	1.113318	2.102804	0.942757	0.550234	0.406542
arginine	175.1	70.1	1	0.698276	0.646552	0.616379	0.698276	0.823276	0.706897	0.728448	0.732759	0.75
histidine	156.1	110.0	1	1.137371	0.638109	0.685377	1.017725	0.967504	0.837518	0.44904	0.691285	0.912851
histidine	156.1	83.2	1	1.125926	0.654815	0.737037	1.081481	0.962963	0.881481	0.47037	0.740741	0.903704
lysine	147.1	84.1	1	1.966667	3.925	5.5	5.041667	0.7475	1.891667	4.2	4.775	4.841667
lysine	147.1	130.1	1	2.503329	5.805593	7.776298	6.977364	0.720373	2.423435	5.938748	6.750999	6.804261
phenylalanine	166.1	120.1	1	0.121359	0.176144	0.382802	0.586685	1.149792	0.117892	0.288488	0.549237	0.643551
phenylalanine	166.1	103.2	1	0.118587	0.175093	0.371747	0.639405	1.171004	0.117472	0.272491	0.572491	0.669145
proline	116.0	70.1	1	1.012848	0.569593	0.563169	0.56531	1.137045	1.143469	0.72591	0.668094	0.736617
proline	116.0	69.0	1	1.005	0.58	0.61	0.585	1.1725	1.1725	0.7375	0.67	0.7375
serine	106.0	60.1	1	0.259637	0.163265	0.384354	0.561224	1.106576	0.1678	0.181406	0.361678	0.479592
serine	106.0	88.0	1	1.791667	1.075	0.496667	0.4825	1.083333	1.616667	0.933333	0.504167	0.489167
tyrosine	182.1	136.1	1	0.272956	0.396855	0.710692	1.08805	1.062893	0.215094	0.596226	0.962264	1.157233
tyrosine	182.1	91.0	1	0.259836	0.379508	0.695082	1.040984	1	0.195902	0.57623	0.95082	1.122951
leucine	147.1	84.1	1	0.266599	0.445352	0.735444	0.827375	1.103166	0.343207	0.657814	0.92237	1.005107
leucine	147.1	130.1	1	0.281642	0.492588	0.790194	0.944128	1.334094	0.358039	0.713797	1.059293	1.163056
glutamate	148.1	84.1	1	1.959248	1.677116	1.137931	0.979624	0.970219	2.194357	1.583072	0.959248	0.768025
glutamate	148.1	130.1	1	1.996454	1.744681	1.166667	1.01773	0.964539	2.241135	1.638298	0.968085	0.776596
tryptophan	205.1	188.2	1	0.221311	0.387705	0.634426	0.728689	1.229508	0.22623	0.591803	0.747541	0.868852
tryptophan	205.1	146.2	1	0.216726	0.37927	0.621908	0.733804	1.13192	0.210836	0.540636	0.69258	0.78563
valine	118.1	72.1	1	0.528689	0.540984	0.840164	1.012295	1.045082	0.721311	0.745902	0.901639	1.069672
valine	118.1	55.0	1	0.527349	0.563815	0.840112	1.025245	1.100982	0.698457	0.729313	0.890603	1.084151
adenine	136.0	119.0	1	0.053901	0.02383	0.020319	0.014681	1.343972	0.021028	0.01195	0.01727	0.012518
adenine	136.0	92.2	1	0.097297	0.024677	0.03114	0.010035	1.351351	0	0.034195	0.016334	0.009318
thymine	127.1	110.0	1	0.159712	0.143885	0.145324	0.152518	0.959712	0.467626	0.118561	0.121439	0.109784
thymine	127.1	109.2	1	1.409483	0.715517	0.398276	0.370259	0.599138	1.168103	0.556034	0.326724	0.30431
homocysteine	136.0	90.0	1	2.445483	2.165109	1.844237	1.725857	1.137072	3.64486	1.657321	0.794393	0.928349
homocysteine	136.0	56.0	1	0.864407	0.819209	0.745763	0.638418	0.59322	1.89548	0.771186	0.29096	0.39548
ornithine	133.1	70.1	1	0.690789	1.927632	3.236842	3.697368	0.75	0.632237	2.828947	4.953947	5.638158

Positive mode, Buffer A: 0.1% formic acid, Buffer B: 0.1% formic acid/100% Methanol

Metabolite	infusion m/z (Q1)	fragment m/z (Q3)	WT SL+0h	WT SL+R 0.5h	WT SL+R 1.5h	WT SL+R 3h	WT SL+R 4.5h	Δ*npr2* SL 0h	Δ*npr2* SL 0.5h	Δ*npr2* SL 1.5h	Δ*npr2* SL 3h	Δ*npr2* SL 4.5h
ornithine	133.1	116.0	1	0.658095	1.971429	3.504762	4.009524	0.857143	0.722857	2.87619	5.266667	6.266667
cytidine	244.1	112.2	1	3.870968	7.067449	4.692082	2.043988	1.175953	4.105572	8.181818	3.665689	1.618768
cytidine	244.1	95.2	1	3.356048	6.575809	4.020443	2.027257	1.187394	4.173765	7.853492	3.713799	1.788756
GMP	364.0	152.0	1	1.339764	1.382637	0.917471	0.685959	1.103966	1.350482	1.393355	0.967846	0.46731
GMP	364.0	135.2	1	1.25	1.459302	0.912791	0.680233	1.014535	1.267442	1.31686	0.927326	0.479651
homoserine	120.0	74.0	1	0.465432	0.382716	0.490123	0.734568	1.962963	0.876543	0.6	0.753086	0.944444
homoserine	120.0	56.2	1	0.445	0.388	0.517	0.734	2.06	0.824	0.56	0.744	0.96
cystathionine	223.1	88.0	1	0.946429	0.227679	0.074821	0.119643	0.910714	0.616964	0.123214	0.071161	0.065893
cystathionine	223.1	134.1	1	0.922481	0.223256	0.089147	0.131783	0.899225	0.631008	0.144186	0.087597	0.074419
SAM	399.1	250.2	1	0.144387	0.117444	0.222798	0.252159	0.949914	0.089983	0.297064	0.283247	0.236615
SAM	399.1	136.0	1	0.14313	0.120992	0.178626	0.287405	0.89313	0.079389	0.306107	0.299618	0.217176
AICAR	258.2	259.1	1	4.223744	9.292237	10.13699	14.31507	0.737443	3.926941	7.305936	12.67123	14.61187
spermidine	146.2	72.1	1	0.446602	0.302913	0.10699	0.112039	1.190291	0.349515	0.231068	0.203883	0.269903
spermidine	146.2	84.0	1	0.318502	0.315419	0.120705	0.120264	1.07489	0.375771	0.218502	0.228194	0.26696
isocitrate	193.0	101.0	1	6.099656	1.975945	1.020619	1.621993	1.142612	7.388316	2.920962	1.786942	3.402062
isocitrate	193.0	83.0	1	5.66474	1.595376	1.028902	2.118497	1.731214	10.17341	4.104046	2.65896	4.855491
succinate	119.0	91.0	1	0.249603	0.38373	0.769841	1.019841	1.027778	0.205556	0.543651	0.936508	1.099206
succinate	119.0	65.0	1	0.360406	0.387817	0.728934	1.006091	1.035533	0.26599	0.592893	0.93401	1.106599
IMP	349.0	137.1	1	0.701449	0.73913	0.663768	0.478261	0.865217	0.646377	0.976812	1.027536	0.495652
IMP	349.0	97.1	1	0.61295	0.689209	0.503597	0.494964	0.815827	0.608633	0.834532	1	0.490647
SAH	385.1	136.2	1	1.255102	2.627551	3.163265	3.571429	0.859694	0.964286	2.984694	3.035714	3.086735
SAH	385.1	134.0	1	1.095368	3.160763	3.378747	3.705722	0.839237	1.152589	3.242507	3.269755	3.351499
citrulline	176.0	159.2	1	1.171171	3.265766	3.783784	2.927928	1.162162	3.175676	7.567568	4.301802	4.594595
citrulline	176.0	70.1	1	0.896552	1.448276	1.491379	1.284483	0.982759	1.603448	2.827586	1.767241	1.862069
hypoxanthine	137.0	110.0	1	1.69086	1.935484	1.5	1.424731	0.908602	1.268817	1.258065	1.053763	1.026882
hypoxanthine	137.0	119.2	1	1.631868	1.82967	1.447802	1.274725	0.851648	1.208791	1.164835	0.961538	1.013736
cytosine	112.0	95.0	1	2.642202	4.211009	2.577982	1.247706	0.93578	2.33945	4.678899	2.018349	0.990826
cytosine	112.0	94.2	1	3.464865	6.378378	3.794595	1.956757	1.318919	4.491892	6.972973	3.010811	1.540541
guanosine	284.0	152.1	1	2.14939	5.243902	4.618902	3.536585	1.018293	1.661585	3.765244	3.155488	2.271341
guanosine	284.0	135.1	1	2.132231	5.165289	4.793388	3.731405	1.028926	1.628099	3.603306	3.144628	2.272727

Metabolite	infusion m/z (Q1)	fragment m/z (Q3)	WT SL+0h	WT SL+R 0.5h	WT SL+R 1.5h	WT SL+R 3h	WT SL+R 4.5h	Δ*npr2* SL 0h	Δ*npr2* SL 0.5h	Δ*npr2* SL 1.5h	Δ*npr2* SL 3h	Δ*npr2* SL 4.5h
Positive mode, Buffer A: 0.1% formic acid, Buffer B: 0.1% formic acid/100% Methanol												
inosine	268.9	137.2	1	1.668224	1.67757	1.359813	1.233645	0.925234	1.14486	1.126168	0.948598	1.004673
inosine	268.9	110.0	1	1.50996	1.74502	1.342629	1.250996	0.836653	1.039841	1.075697	0.928287	1
thymidine	243.0	127.2	1	0.798701	0.857143	0.766234	0.636364	1.006494	0.733766	1.376623	0.922078	0.503247
uridine	245.0	112.9	1	1.621469	5.564972	7.740113	8.983051	1.090395	1.601695	6.045198	7.740113	7.40113
dAMP	332.1	81.0	1	1.691803	0.760656	0.29377	0.261967	0.777049	1.344262	0.616393	0.370492	0.291475
CMP	324.1	112.2	1	1.020349	0.965116	0.642442	0.34593	0.901163	0.924419	0.875	0.430233	0.2375
deoxyadenosine	252.1	136.2	1	0.941176	0.662185	0.540336	1.042017	1.117647	1.184874	0.857143	0.94958	1.243697
cystine	240.9	74.0	1	1.19322	1.511864	2.172881	3.101695	2.633898	1.237288	1.762712	2.261017	3.013559
agmatine	131.1	72.1	1	0.536458	1.536458	0.33125	0.35625	1.578125	0.822917	0.619792	0.323958	0.358333
putrescine	89.1	72.0	1	0.024257	0.021188	0.015743	0.009465	0.748515	0.046436	0.015446	0.013762	0.010792
Negative mode, Buffer A: 5mM Tributyl amine, Buffer B: 100% Methanol												
2,3-dihydroxybenzoate	185.0	78.9	1	0.851449	0.862319	0.657609	0.576087	0.702899	0.677536	0.650362	0.554348	0.476449
2,3-dihydroxybenzoate	185.0	96.9	1	0.42268	0.604811	0.620848	0.431844	0.250859	0.468499	0.463918	0.32646	0.365407
3-phosphoglycerate	426.0	78.8	1	2.766355	2.009346	1.018692	0.248598	1.345794	2.869159	1.224299	0.228037	0.303738
3-phosphoglycerate	426.0	158.9	1	2.825429	2.088799	1.039354	0.268416	1.412714	2.986882	1.331988	0.225025	0.323915
ADP	144.9	100.9	1	0.703297	1.016484	1.401099	1.417582	1.340659	0.978022	2.208791	2.225275	1.340659
ADP	144.9	56.8	1	0.709163	0.968127	1.262948	1.25498	1.203187	0.900398	1.521912	1.689243	0.928287
cis-aconitate	172.9	85.0	1	1.197991	1.002869	1.097561	1.428981	1.018651	1.124821	1.109039	1.578192	2.711621
cis-aconitate	172.9	129.0	1	1.12517	0.907483	1.040816	1.387755	0.945578	1.021769	1.009524	1.428571	2.380952
citrate	191.0	110.9	1	1.13879	1.088968	1.039146	1.170819	1.151839	1.061684	1.233689	1.364176	1.43535
citrate	191.0	87.0	1	1.1606	1.130621	1.139186	1.1606	1.263383	1.077088	1.244111	1.372591	1.518201
CoA	766.2	79.1	1	1.179562	1.985401	1.032117	0.744526	1.157664	1.426277	2.248175	4.175182	2.087591
CoA	766.2	408.0	1	0.987952	0.329317	0.919679	1	0.7751	1.15261	2.39759	3.558233	1.39759
dihydroxyacetonephosphate	168.9	96.9	1	0.670418	0.985531	0.691318	0.445338	1.16881	0.942122	1.255627	0.580386	0.519293
dihydroxyacetonephosphate	168.9	78.9	1	0.658354	0.852868	0.591022	0.406484	1.13217	0.845387	1.15212	0.528678	0.508728
fructose-1,6-bisphosphate	338.9	78.8	1	0.532468	0.71645	0.848485	0.896104	1.214286	0.74026	1.255411	0.950216	0.681818
fructose-1,6-bisphosphate	338.9	96.8	1	0.498099	0.794677	1.053232	1.18251	1.068441	0.714829	1.444867	1.34981	0.737643
fructose-6-phosphate	258.9	78.9	1	0.351341	0.735632	1.429119	1.551724	1.318008	0.440613	1.685824	2.455939	1.40613
fructose-6-phosphate	258.9	169.0	1	0.302069	0.82069	1.593103	1.662069	1.331034	0.412414	1.834483	2.77931	1.475862

Positive mode, Buffer A: 0.1% formic acid, Buffer B: 0.1% formic acid/100% Methanol

Metabolite	infusion m/z (Q1)	fragment m/z (Q3)	WT SL+0h	WT SL+R 0.5h	WT SL+R 1.5h	WT SL+R 3h	WT SL+R 4.5h	Δ*npr2* SL 0h	Δ*npr2* SL 0.5h	Δ*npr2* SL 1.5h	Δ*npr2* SL 3h	Δ*npr2* SL 4.5h
fumarate	114.9	71.1	1	0.752988	0.780876	0.816733	0.804781	0.768924	0.689243	0.669323	0.713147	0.63745
fumarate	114.9	70.0	1	0.707921	0.747525	0.811881	0.811881	0.821782	0.678218	0.707921	0.80198	0.678218
glucose-6-phosphate	258.9	97.0	1	0.26391	0.618045	1.473684	1.541353	1.578947	0.474436	1.954887	3.556391	1.917293
glucose-6-phosphate	258.9	199.0	1	0.32625	0.81875	1.66875	1.65	1.3875	0.4425	1.9	2.8875	1.58125
isocitrate	191.0	111.0	1	1.051282	1.102564	1.076923	1.136752	1.034188	1.094017	1.042735	1.401709	1.230769
isocitrate	191.0	73.0	1	2.537859	1.154047	1.56658	3.420366	1.349869	4.334204	3.211488	3.733681	7.075718
lactate	88.9	43.0	1	0.378917	0.529915	0.723647	0.680912	1.31339	0.554131	0.774929	0.578348	0.347578
lactate	88.9	71.1	1	0.425856	0.621673	0.78327	0.769962	1.391635	0.596958	0.792776	0.604563	0.395437
malate	132.9	114.9	1	0.362909	0.592727	0.730909	0.967273	1.341818	0.821818	0.989091	1.167273	0.996364
malate	132.9	71.0	1	0.347863	0.580342	0.722222	0.982906	1.358974	0.792308	1.034188	1.213675	1.034188
NADP+	742.1	620.2	1	1.603376	2.053446	1.954993	0.969058	1.067511	1.389592	3.516174	1.729958	0.464135
NADP+	742.1	78.9	1	1.006912	1.211982	1.211982	0.910138	1.179724	1.0553	2.004608	1.138249	0.465438
nicotinic acid	121.9	78.0	1	0.846154	1.015385	0.984615	0.876923	0.887179	0.917949	0.697436	0.784615	0.779487
orotate	154.9	110.9	1	0.775109	0.790393	0.842795	0.764192	0.69214	0.652838	0.598253	0.582969	0.543668
oxaloacetate	130.9	87.0	1	0.453649	0.378698	0.56213	0.433925	1.216963	0.87574	0.90927	0.633136	0.357002
phosphoenoylpyruvate	166.9	78.9	1	2.803922	2.068627	1.058824	0.176471	0.905882	2.764706	0.839216	0.095392	0.166667
6-phosphogluconate	274.9	78.9	1	2.005242	1.120577	0.475754	0.120446	1.454784	3.420708	0.880734	0.251638	0.258191
6-phosphogluconate	274.9	97.0	1	1.680162	0.77834	0.382591	0.111336	1.38664	3.147773	0.742915	0.282389	0.266194
ribose-5-phosphate	228.9	79.1	1	1.87602	1.445351	0.96248	0.644372	1.03752	2.300163	1.192496	2.593801	1.473083
ribose-5-phosphate	228.9	96.9	1	1.764706	1.186791	0.914345	0.510836	1.114551	2.198142	1.073271	0.94324	1.331269
shikimate	172.9	93.0	1	0.627208	0.584806	1.136042	0.45583	0.95583	2.137809	3.339223	2.279152	0.848057
alanine	88.0	88.0	1	0.859107	0.819588	0.838488	0.816151	0.695876	0.695876	0.637457	0.647766	0.546392
glycine	74.0	74.0	1	1	0.953271	0.705607	0.711215	0.872897	0.701869	0.704673	0.690654	0.656075
ATP	507.0	79.0	1	1.904	2.96	4.976	7.2	7.752	8.48	15.68	19.28	30.16
succinate	116.9	73.0	1	0.343866	0.414498	0.607807	0.494424	2.026022	0.401487	0.726766	0.89777	1.066914
succinate	116.9	99.0	1	0.340704	0.396985	0.594975	0.535678	2.201005	0.38593	0.733668	0.919598	1.105528
pyruvate	86.9	86.9	1	0.871429	0.871429	0.885714	0.814286	0.728571	0.714286	0.65	0.666429	0.557143
pyruvate	86.9	43.0	1	1.010606	0.933333	0.468182	0.827273	1.112121	0.510606	0.827273	0.681818	0.792424
leucine	130.0	84.0	1	0.503356	1.043624	3.926174	5.234899	4.496644	0.24094	2.681208	7.986577	10.63758
isoleucine	130.0	82.1	1	0.093467	0.532663	1.673367	2.477387	1.633166	0.30402	1.366834	3.648241	3.939698

Positive mode, Buffer A: 0.1% formic acid, Buffer B: 0.1% formic acid/100% Methanol												
Metabolite	**infusion m/z (Q1)**	**fragment m/z (Q3)**	**WT SL+0h**	**WT SL+R 0.5h**	**WT SL+R 1.5h**	**WT SL+R 3h**	**WT SL+R 4.5h**	**Δ*npr2* SL 0h**	**Δ*npr2* SL 0.5h**	**Δ*npr2* SL 1.5h**	**Δ*npr2* SL 3h**	**Δ*npr2* SL 4.5h**
isoleucine	130.0	45.2	1	0.210938	0.517969	2.226563	2.460938	1.679688	0.369531	1.195313	2.804688	4.023438
glutamine	144.9	127.2	1	2.770053	15.18717	51.22995	47.00535	0.59893	3	23.15508	54.54545	56.14973
glutamine	144.9	109.0	1	2.77533	14.75771	48.89868	48.34802	0.669604	3.237885	23.78855	52.86344	54.95595
lysine	144.9	97.0	1	0.591654	5.33532	16.84054	17.58569	0.800298	1.351714	8.435171	18.33085	20.11923